MET-2 AND SET-25 HAVE SEXUALLY DIMORPHIC EFFECTS ON CHROMOSOME STRUCTURE IN *CAENORHABDITIS ELEGANS*

by

Wing Nam Fung (Lacole)

A thesis submitted to the Faculty of the University of Delaware in partial fulfillment of the requirements for the degree of Master in Science in Biological Sciences

Winter 2023

© 2023 Wing Nam Fung
All Rights Reserved

MET-2 AND SET-25 HAVE SEXUALLY DIMORPHIC EFFECTS ON CHROMOSOME STRUCTURE IN *CEANORHABDITIS ELEGANS*

by

Wing Nam Fung (Lacole)

Approved:_____
Aimee Jaramillo-Lambert, Ph.D.
Professor in charge of thesis on behalf of the Advisory Committee

Approved:_____
Velia Fowler, Ph.D.
Chair of the Department of Biological Sciences

Approved:_____
John A Pelesko, Ph.D.
Dean of the College of Arts and Sciences

Approved:_____
Louis F. Rossi, Ph.D.
Vice Provost for Graduate and Professional Education and
Dean of the Graduate College

ACKNOWLEDGEMENTS

I would like to acknowledge and express my deepest appreciation to Dr. Aimee Jaramillo-Lambert for her continuous guidance and support throughout my graduate study and research. Her patience, motivation, enthusiasm and immense knowledge have deeply inspired me and shaped my growth.

I would also like to express my sincere gratitude to my committee members, Dr. Lisha Shao and Dr. Jeffrey Caplan, for the support, encouragement and insightful comments. Thank you for your constructive feedback that has led me in the right direction with the research and project.

Many thanks to my current lab members, Nirajan, Kent, Christine, Shannon, Darline, Tuyaa, Gabby, Hiski, Lauren (Stewart), and to my former lab members, Nancy, Alekya, Deonna, Lauren (Salvitti), Chris for their wonderful support and collaboration, which have tremendously improved my research and graduate study experience.

Finally, I am very grateful for my family and friends, who have always been there and supported me through all the ups and downs no matter where they are. Without their endless love, unconditional support and understanding, it would not have been possible.

TABLE OF CONTENTS

LIST OF FIGURES..... vi
ABSTRACT..... vii

Chapter

1. INTRODUCTION..... 1

1.1 Meiosis..... 1
1.2 *Caenorhabditis elegans* as a Model Organism to Study Meiotic Processes.. 3

1.2.1 The Genome and Genetics of *Caenorhabditis elegans* 6
1.2.2 *Caenorhabditis elegans* Germlines 8

1.3 Histone Modification - Methylation..... 10
1.4 Preliminary Data: MET-2 and SET-25 are Differentially Required for Meiotic Chromosome Structure in Oogenesis vs. Spermatogenesis..... 12
1.5 Proposed Hypothesis and Research Aims..... 15

2. **MATERIALS AND METHODS**..... 17

2.1 *C. elegans* Strains and Maintenance 17
2.2 Embryonic Viability Assay..... 17
2.3 Immunistaing and DAPi Staining..... 18
2.4 Image Collection, Processing and Measurement 19

3. RESULTS 21

3.1 Loss of MET-2 and SET-25 Does Not Affect Progeny Viability..... 21
3.2 The Combined Loss of Both MET-2 and SET-25 Results in an Increase of Chromosome Bivalent Length in Spermatogenesis and Oogenesis..... 26
3.3 Loss of Both MET-2 and SET-25 Does Not Affect Progeny Viability..... 27
3.4 H3K9me2 Does Not Localize on Diakinesis Chromosomes in the Germline of Males and Hermaphrodites…….. 28
3.5 Loss of MET-2 Does Not Affect the Conversion of H3K9me3 at Diakinesis……. 29
3.6 The Switch Off of Global Transcription is Delayed in *met-2(n4256)* Spermatogenesis..... 31

4. **DISCUSSION**..... 33

4.1 Defects in Chromosomal Structure and Compaction in MET-2 and SET-25 mutants..... 33

4.2 Histone Methyltransferase MET-2 is Essential for Embryonic Performance..... 37
4.3 Step-wise Methylation of H3K9 May Not be Present in *C. elegans* Germline 38
4.4 MET-2 is important for the chromosome condensation at the karyosome in spermatocytes…….…… 39
4.5 Conclusion..... 40

REFERENCES 42

Appendix

A PREVIOUS WORK ON HTAS-1 AND HCP-6 48

LIST OF FIGURES

Figure 1.1: *C. elegans* life cycle from embryo to adult stage at optimal growth conditions……... 6

Figure 1.2: Spatiotemporal layout and morphological structure of the *C. elegans* germline……... 10

Figure 1.3: Diakinesis bivalent length is smaller in *C. elegans* male……..... 13

Figure 1.4: Histone post-translational modifications differentially affect oocyte and spermatocyte bivalent length in *C. elegans*. ……...…… 15

Figure 3.1: *met-2(n4256)* reduces embryonic viability in hermaphrodites….……..… 22

Figure 3.2: *met-2(n4256)* reduces brood size in hermaphrodites.…..……..….. 23

Figure 3.3: Embryonic viability of *met-2(n4256)* hermaphrodites is rescued by mating to wild-type males……..…….…. 24

Figure 3.4: Loss of both MET-2 and SET-25 in spermatogenesis does not affect embryonic viability at 20℃…….……..... 25

Figure 3.5: Loss of SET-25 has no effect on embryonic viability in spermatogenesis at 24℃……..……... 25

Figure 3.6: *met-2(n4256); set-25(n5021)* Bivalent Length Increases in Both Oogenesis and Spermatogenesis……... 27

Figure 3.7: H3K9me2 is not detectable on chromosomes within diakinesis nuclei of all strains..…… 29

Figure 3.8: H3K9me3 is strongly detected on all the chromosomes of diakinesis nuclei in both oogenesis and spermatogenesis……... 30

Figure 3.9: Delayed switch off of global transcription in *met-2(n4256)* mutant male.. 32

Figure A.1: Loss of HTAS-1 does not affect embryonic viability.…...……..…… 49

Figure A.2: Loss of *hcp-6(mr17)* causes a reduction in embryonic viability at 24℃... 50

Figure A.3: H3K9me2 is detected on chromosomes within pachytene in spermatogenesis ……. …….. 51

ABSTRACT

Meiosis is a highly conserved cellular division, which allows for the formation of haploid gametes. During meiosis chromosomes undergo two successive segregation events. Homologous chromosomes segregate in meiosis I and the sister chromatids subsequently segregate in meiosis II, leading to the production of egg and sperm with half the number of chromosomes of the parent cells. Although many similarities exist between meiosis in males and females, there are also meiotic mechanisms that differ between oogenesis and spermatogenesis. In *C. elegans*, we found that the bivalent length of diakinesis oocytes is significantly longer than spermatocytes. In addition, we found that mutations in different genes involved in histone post-translational modifications have distinct impacts on oocyte and spermatocyte bivalent length. A mutation of *set-25*, a histone methyltransferase converting histone H3 lysine 9 dimethylation (H3K9me2) to trimethylation (H3K9me3), reduces the bivalent length in oocytes. On the other hand, a mutation of *met-2*, a histone methyltransferase depositing H3K9me2 in the germ line decreases the bivalent length in spermatocytes. Although bivalent length is altered in these mutants, I discovered that there is no significant impact on embryonic viability. Because the epigenome is complex there could be redundant mechanisms to prevent germline dysfunction. Analysis of a *met-2(n4256) set-25(n5021)* double mutant, which have previously been found to interact genetically, resulted in a significant increase in diakinesis bivalent length compared to wild type and the single mutants. Through immunostaining against histone H3 lysine 9 dimethylation and trimethylation, we found robust localization of H3 lysine 9 trimethylation at diakinesis nuclei in both spermatogenesis and oogenesis, but H3

lysine 9 dimethylation is absent at diakinesis in both hermaphrodite and male germlines. Analysis of global gene transcription in spermatogenesis with an antibody against an active form of RNA polymerase II revealed that a delay in the silencing of global transcription occurs in *met-2(n4256)*. These findings have revealed that two histone methyltransferases, MET-2 and SET-25, have differential roles on chromosome compaction and structure in *C. elegans* oogenesis and spermatogenesis.

Chapter 1

INTRODUCTION

1.1 Meiosis

Meiosis is a highly conserved cellular division utilized by sexually reproducing organisms to pass on genetic material to offspring through the formation of haploid gametes, such as egg and sperm. The production of haploid gametes (half the number of chromosomes as the parental cell) is accomplished by one round of DNA replication followed by two consecutive rounds of chromosome segregation, which are called meiosis I and meiosis II. In meiosis, homologous chromosomes segregate away from each other at meiosis I, while sister chromatids segregate towards the opposite poles of the spindle during meiosis II. Meticulous regulation of meiotic events are required for the production of haploid gametes. When chromosomes are unable to segregate properly the result is the production of gametes with incorrect chromosome numbers (aneuploidy). Aneuploidy in humans can lead to infertility, birth defects and miscarriages (Cahoon and Libuda, 2019).

Before entering meiosis, the cell undergoes DNA synthesis called S-phase in which the genetic material is duplicated. During this process, each chromosome undergoes replication to generate sister chromatids with identical genetic content and where the sister chromatids are connected by cohesin (Lodish et al., 2016). The total DNA content increases from 2n to 4n. Once S phase is completed, the cell enters meiosis I with an extended prophase stage, which can be defined by five sub-stages, leptotene, zygotene, pachytene, diplotene, and diakinesis. In the first stage, leptotene, the chromosomes condense by reorganizing themselves into a loop-axis DNA

structure where loops of DNA extend out from a chromosome axis. Meiotic recombination is also initiated by the formation of DNA double-strand breaks (DSBs) (Grey and de Massy, 2021). The second stage of meiotic prophase I is zygotene where homologous chromosomes begin to pair and associate with each other in a process called synapsis. Synapsis is mediated by a multi-protein complex, the synaptonemal complex (SC), which is assembled in between the paired homologous chromosomes (Pawlowski and Cande, 2005; Lodish et al., 2016). The SC acts as a scaffold that allows the interaction between homologous chromosomes. After zygotene is the pachytene substage of meiotic prophase I. At this stage homologous chromosomes are fully synapsed and meiotic recombination occurs. The SC facilitates the formation of crossovers that involves swapping the genetic material between the homologous chromosomes. Following pachytene is diplotene where synapsis ends with the disassembly of synaptonemal complex; nonetheless, the homologous chromosomes remain paired by physical linkages called chiasmata. Chiasmata are important for proper segregation of homologous chromosomes at the first meiotic division (Hirose et al., 2011). Diakinesis is the last stage of prophase – chromosomes become highly condensed and remodel to promote formation of a bivalent, where a pair of homologous chromosomes are physically held together through a crossover (Azumi et al., 2002). Following meiotic prophase I, homologous chromosomes align on the equator of the cell called the metaphase plate (metaphase I). Subsequently in anaphase I, homologous chromosome segregation is achieved by the cleavage of cohesin on the chromosome arms by separase. Cohesins at centromeres are protected such that sister chromatids are still connected, but homologous chromosomes are pulled toward the

spindle pole via kinetochore microtubule shortening at the spindle pole end (Forer and Wilson, 2000). At the last stage of the first meiotic division, telophase I, the separated homologs arrive at opposite spindle poles followed by cytokinesis, which divides the cytoplasm into two individual haploid daughter cells.

Meiosis II resembles mitosis as sister chromatids are separated, yet meiosis II yields daughter cells containing a single set of chromosomes instead of the two sets of chromosomes of a diploid cell. In meiotic prophase II, chromosomes within the haploid daughter cells from the first meiotic division become condensed, and a new set of spindle fibers begins to form. The chromosomes move toward the center of the cell and align at the metaphase plate. Once the alignment is completed, cohesin complexes at the centromeres are cleaved by separase, and the meiotic spindle fibers start to pull the sister chromatids apart toward the opposite end of the cells (Brooker and Berkowitz, 2014). At the final phases of the second division – telophase II and cytokinesis II, the nuclear envelope reassembles as the individual chromatids reach the poles of each cell, and the cytoplasm is divided into two haploid daughter cells. The entire meiotic second division yields four daughter cells containing half the genetic material as the parental cell (Lodish et al., 2016).

1.2 *Caenorhabditis elegans* as a Model Organism to Study Meiotic Processes

The nematode *Caenorhabditis elegans* is a free-living organism that are usually found living in humid areas rich in microbes, such as areas with decaying vegetation (e.g. vegetable gardens and farms) (Schulenburg and Félix, 2017). Therefore, bacteria, which are easily found in rotting plants, in particular *Escherichia coli* (*E. coli*), become

their main food source (Barriere and Felix, 2014). In 1963, Sydney Brenner, a biologist from South Africa, first established *Caenorhabditis elegans* as an exceptional model organism for studying animal development and behavior because of its size, life cycle, and ease of laboratory cultivation (Riddle et al., 1997). It also becomes a powerful model to use in genetic analysis due to a rapid life cycle, body transparency, hermaphroditic self-fertilization, and a large number of progeny.

This tiny nematode exists as two sexes, hermaphrodites and males, that can be genetically distinguished by the sex chromosomes. They can be cultured in agar petri-plates seeded with *E. coli*, and cells can be simply observed through a general dissecting microscope due to its transparent cuticle. The cultivation temperatures range for *C. elegans* from 12°C to 25°C in the laboratory (Klass, 1977; Wu et al., 2009; Xiao et al., 2013). The lifespan of *C. elegans* is two to three weeks at 20 °C, which is considered an optimal temperature for growth. *C. elegans* can also be frozen and stored at -80°C indefinitely. Under normal conditions, the life cycle of *C. elegans* is completed in about 3 days, and is comprised of three main developmental stages, embryonic stage, larval stages (L1 to L4), and reproductive adulthood (**Figure 1.1**).

After fertilization, the one-cell zygote undergoes a series of mitotic cleavages during embryogenesis and hatches within 9 hours from the embryo being laid at 30-cell stage. After hatching, L1 larvae continue to grow and molt through cuticles thickening into the L2 stage, and then into L3 and then L4. The final molting is from L4 larvae to young adult, which then develops into a reproductive adult. The L4 larvae stage is an important stage for the reproductive system of *C. elegans* where spermatogenesis and oogenesis initiate. However, the life cycle of *C. elegans* is hugely sensitive to the

change of environmental factors, which can influence the growth rate of *C.elegans* in its developmental stages. *C. elegans* can arrest at an alternative specific developmental stage called the dauer diapause, which is a long-lived stress resistant stage to prevent dehydration under unfavorable external conditions, including extreme temperatures, lack of food, and overcrowding (Fielenbach and Antebi, 2008). To observe a dauer diapause formation in the laboratory, *C. elegans* has to undergo the initiation of larval development on an agar plate with limited food source. Instead of entering the dauer diapause stage, if embryo hatches into the environment without food, they fail to initiate larval development and arrest at the L1 diapause. Just like frozen larvae, dauer larvae can be potentially recovered to reproductive adults with a normal life span by reinstalling favorable environmental factors.

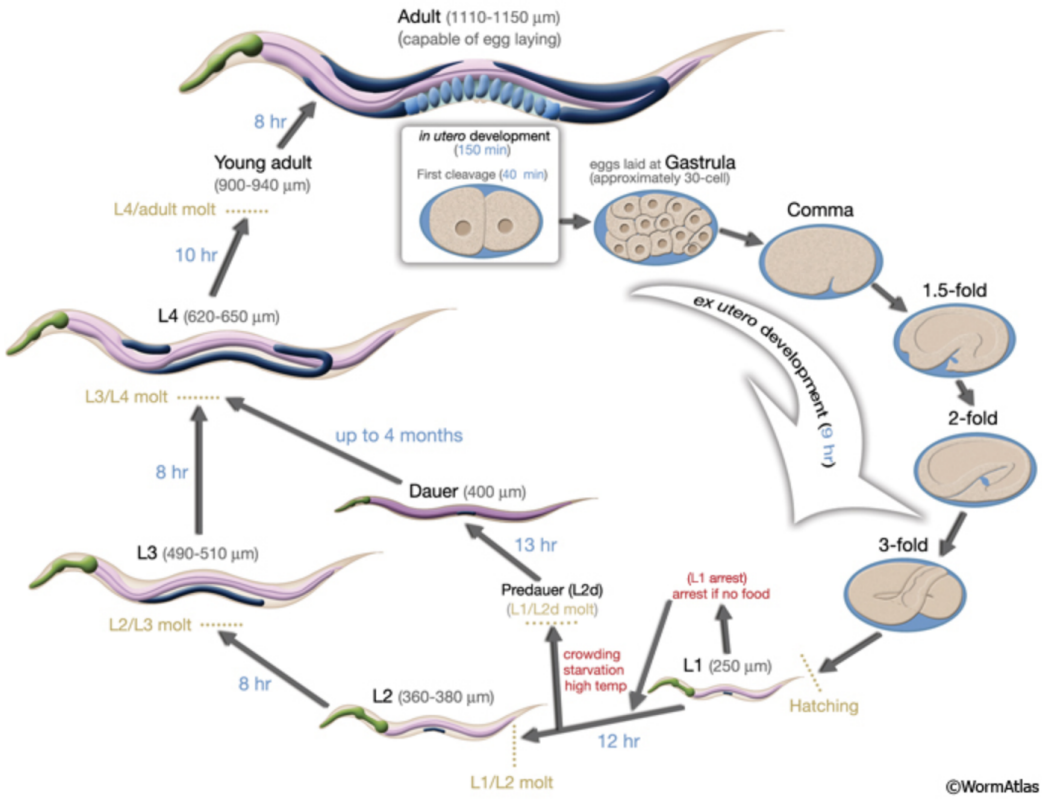

Figure 1.1 *C. elegans* Life Cycle from Embryo to Adult Stage at Optimal Growth Conditions. *C. elegans* has a rapid embryogenesis and hatches after 14 hours. After hatching, they undergo four larvae developmental stages (L1-L4). At the L2 stage, worms can arrest at a specific third developmental stage called the dauer diapause when abnormal environmental conditions are present. When optimal environmental conditions are reinstalled, dauers can re-enter the normal life cycle. *C. elegans* sexes can be distinguished at the L4 stage where the U-shape gonad is completely developed. Spermatogenesis occurs throughout the males lifespan and at the L4 stage in hermaphrodites, which switch to oogenesis in adulthood. Image from Altun et al., 2021.

1.2.1 The Genome and Genetics of *Caenorhabditis elegans*

In 1998, the first entire genome sequence of multicellular organisms, *Caenorhabditis elegans,* was sequenced within the six pairs of chromosomes. Hermaphrodites have five autosomal pairs and one pair of sex chromosomes (two X chromosomes - XX), while males contain five autosomal pairs and only one sex chromosome (one X chromosome - XO) (Riddle et al., 1997). The difference in X chromosome number leads to a sex imbalance situation in nature where the majority of *C. elegans* offspring are hermaphrodites, while only 0.1–0.2% of the progeny are males, which arise through rare meiotic nondisjunction of the sex chromosomes (Corsi et al., 2015). *C. elegans* shares nearly 83% (around 15,344 sequences) of their proteome with humans, and over 7000 genes have matching human gene transcripts (Lai et al., 2000). This makes *C. elegans* a powerful tool to approach molecular biology and genetics.

C. elegans hermaphrodites are capable of self-fertilization by producing both spermatocytes and oocytes. Hermaphrodites produce around 300 sperm at the last larvae stage of development, L4, but they switch to producing oocytes throughout their adult life span. Hermaphroditic self-fertilization is the primary mode of *C. elegans* reproduction. In contrast, males continuously produce spermatocytes over their

lifetime. Unmated hermaphrodites maximally produce about 300 progeny, while mating hermaphrodites with males produces cross-progeny, and enhances the reproductive performance by increasing the progeny from 300 to around 1000 (Corsi et al., 2015). Mating hermaphrodites and males is a useful method for rescuing mutations. For instance, the offspring of homozygous hermaphrodite with a visible recessive mutant phenotype crossed with a wild-type male do not show the mutant phenotype. Mutant hermaphrodites with spermatocyte defects, which results in sterility, can also be rescued by the introduction of wild-type sperm from males through mating.

C. elegans is a great model organism for the use of an experimental technique called forward genetics, which involves mapping of phenotypic variation based on genotypes, due to the ease of recovery of homozygous mutations through hermaphrodite self mating (Corsi et al., 2015; Gao et al., 2018). This process begins with the induction of genomic mutations through the exposure of adult hermaphrodite worms to ethane methylsulfonate (EMS). EMS is an alkylating reagent that is commonly utilized for genetic screening, especially for forward genetics screening. EMS induces guanine alkylation, which results in transition mutations by mispairings with thymine in DNA replication (Snyman et al., 2021). Besides single nucleotide mutations, EMS is also capable of causing insertions and deletions of DNA sequences. After EMS mutagenesis, the phenotype of interest is screened for among the progeny and the role of the mutated gene determined by comparison to wild-type animals (Gao et al., 2018). In addition to a genetic cause of an altered or abnormal phenotype introduced by a chemical mutagenesis (Forward genetics), another strategy is reverse genetics, which focuses on the phenotypic impact of the alteration of specific target

genes (Gao et al., 2018). This approach can be achieved by transient gene knockdown/gene silencing. RNA interference (RNAi) is one of the reverse genetics methods, which can be easily incorporated into the *C.elegans* food source - bacteria. Another reverse genetics method is genome editing through CRISPR/Cas 9.

1.2.2 *Caenorhabditis elegans* Germlines

In *C. elegans*, the germline is housed in the gonad. The arms of the gonad are determined by somatic gonad precursors Z1/Z4 dividing during larval development. Somatic gonad precursors at both ends of gonad primordium divide to produce 143 cells in hermaphrodites, yet only one somatic gonad precursor divides in male to generate 56 cells (Riddle et al., 1997). The major structural distinction between hermaphrodites and males is the U-shape gonad in which hermaphrodites have two symmetric U-shape gonads and males only have a single gonad (**Figure 1.2**). Germline mitotic proliferation occurs at the distal end of the U-shaped gonad, which is regulated through the notch signaling pathway. Each distal end of the hermaphrodite gonad is capped by a single somatic cell called the distal tip cell, which is responsible for the production of the delta-like ligand, LAG-1 (Seidel et al., 2018). GLP-1, a notch family receptor located on the surface of the germ cells in the proliferative zone, negatively regulates germ cells from entering meiosis in response to LAG-1 throughout the developmental larvae stages to adulthood. As mitotic germline nuclei progress along the proximal proliferative zone, markers of differentiation, such as GLD-1, are increasingly expressed (Seidel et al., 2018). Once germ cells arrive at the transition zone meiotic differentiation begins. As previously mentioned, chromosomes undergo a

series of sub-stages of meiotic prophase I and all substages can be observed in the C. elegans germline as it is arranged in a spatio-temporal order within the gonad syncytium with the early stages at the distal end and the later stages at the proximal end. At the most proximal end of the gonad arm the chromosomes become more condensed at diakinesis, which is referred to as the condensation zone. Spermatogenesis at the condensation zone varies from oogenesis in requiring an extra stage – karyosome formation where a cluster of chromosomes forms with a compact spherical structure (Shakes et al., 2009).

Meiosis of hermaphrodites occurs from the late L4 stage to adulthood. As previously mentioned, spermatogenesis occurs during the L4 stage of larvae development, and oogenesis takes over once adulthood is reached. Each hermaphrodite gonad generates nearly 150 amoeboid sperm. Inactive hermaphrodite sperm activates to a motile form as they pass through a chamber called the spermatheca, which also functions as a sperm storage area adjacent to the uterus (Shakes, 2011). Fertilization takes place as an individual oocyte enters the spermatheca and fuses with an active sperm. Contrarily, a spermatheca does not exist in the male gonad, the sperm remains in an inactivated form within the seminal vesicle until the process of ejaculation (Smith and Stanfield, 2012). Male sperm are relatively larger than hermaphrodite sperm and are capable of outcompeting hermaphrodite sperm as it migrates from the vulva to the spermatheca after insemination.

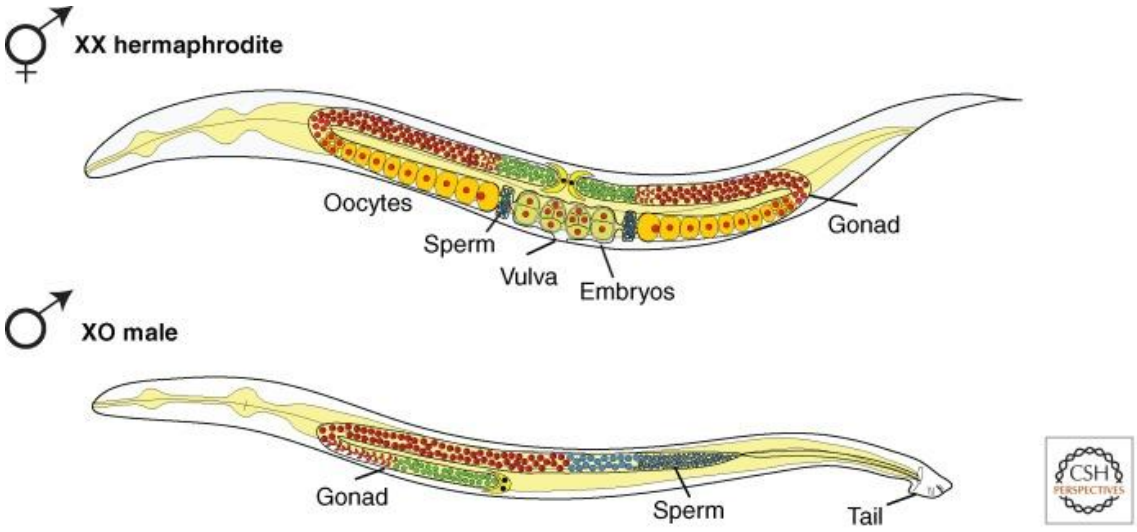

Figure 1.2: Spatiotemporal Layout and Morphological Structure of the *C. elegans* Germline. Morphological structure of hermaphrodite (top) and male (bottom) gonads. Specific structures of hermaphrodites reproductive tract: spermatheca and vulva; Male specific mating structure: tail (Strome et al., 2014).

1.3 Histone Modifications - Methylation

In eukaryotic cells, histones have an important role in the regulation and organization of chromatin and gene expression. A length of chromosomal DNA is packed with the assistance of four core histones (two each of H2A, H2B, H3, and H4) to form a complex called a nucleosome (Mariño-Ramírez et al., 2005). The histone octamers in *C. elegans* are highly conserved. It is also relatively similar to the structure of human histones with 80% identical amino acids in sequence (H3 and H4 are 97% and 98% identical to those of humans) (Cui and Han, 2007). Due to the similarity of histone structure, *C. elegans* is an excellent model organism to study histone modifications.

Transcriptional gene expression can be controlled by the differential organization of chromatin into euchromatic and heterochromatic forms (Morrison and Thakur, 2021). Euchromatin is transcriptionally active chromatin, which is enriched in

genes; on the other hand, heterochromatin is considered a condensed state preventing access to the genes. Histone modification is the main factor to determine the organization of the chromatin by modifying the interaction between nucleosome–nucleosome or nucleosome–DNA by changing the charge of the highly basic histone tail as well as disrupting the contact sites between DNA and the nucleosomal core particle. There are various histone modifications, including both acetylation and methylation of lysines and arginines, ubiquitylation of lysine, phosphorylation of serines and threonines, and sumoylation of lysines, and they all target the residues on the N-terminal tail of the histones (Bowman and Poirier, 2015)

Histone methylation is one of the most common histone post-translational modifications (PTMs). A methyl group is deposited on the basic residues of histones H3 and H4 subunits, such as arginine, lysine, and histidine. Arginine methylation tends to facilitate gene expression, yet lysine methylation engages in both activation and repression of gene expression depending on which residue site the methylation occurs (Greer et al., 2012). For example, methylation of lysine 4 and lysine 36 on the N-terminal tail of histone H3 promotes transcriptional activation, whereas the addition of a methyl group on lysine 9 or lysine 27 fosters the repression of gene expression (Bessler et al., 2010). Furthermore, in addition to the methylation site, the degree of methylation at one particular site can also contribute to the activation and repression of gene expression (Jih et al., 2017; Kaukonen et al., 2020). Histone H3 lysine 9 dimethylation (H3K9me2) is heavily related to facultative heterochromatin. Conversely, histone H3 lysine 9 trimethylation (H3K9me3) silences gene expression (Peters et al., 2003).

The multiplicity of methylations to different degrees as well as residues is governed by a variety of histone methyltransferases. A human SETDB1 homolog histone methyltransferase, MET-2, deposits methyl groups on lysine 9 of histone H3 and is specifically required for the presence of H3K9me2 in the germ line (Loyola et al., 2006; Bessler et al., 2010). MET-2 is classified as a histone mono/di-methyltransferase because it is responsible for the addition of the first and second methyl groups of Histone H3 at lysine 9 in the cytoplasm (Huang et al., 2022; Towbin et al., 2012). SET-25 is one of the members of the SET domain proteins, which mediate the conversion of histone H3 lysine 9 dimethylation (H3K9me2) to trimethylation (H3K9me3) (Towbin et al., 2012). Interestingly, *set-25* mutants exhibit phenotypes similar to wild type worms (Woodhouse et al., 2018). It has been proposed that a stepwise methylation on H3K9 occurs through a sequential relationship between MET-2 and SET-25 in which addition of H3K9me1/2 by cytoplasmic MET-2 is followed by conversion of H3K9me3 by SET-25 within the nucleus (Towbin et al., 2012; Padeken et al., 2019).

1.4 Preliminary Data: MET-2 and SET-25 are Differentially Required for Meiotic Chromosome Structure in Oogenesis vs. Spermatogenesis.

Although spermatogenesis and oogenesis are the meiotic processes that produce haploid gametes containing a complete set of genetic material for fertilization and the formation of a diploid organism, their products are very distinct in terms of morphology, motility and function (Spiller et al., 2017). Differences in the formation of spermatozoa and oocytes is revealed by various mechanistic dissimilarities. In many species, the timing of haploid gamete development between spermatogenesis and

oogenesis is different, where spermatogenesis occurs throughout the adult male lifespan while oogenesis is arrested at certain stages in some organisms. Likewise, spermatids in *C. elegans* males are produced throughout adult life and are stored in the seminal vesicle, while hermaphrodites only produce limited oocytes over the adult lifetime (L'Hernault and Roberts, 1995; Andux and Ellis, 2008). The morphologies of the products between oogenesis and spermatogenesis, egg and sperm, are also distinct. An oocyte arises from chromosomes that undergo asymmetric divisions to produce one haploid ovum, while four haploid spermatocytes of equal size are generated from the chromosomes undergoing symmetric divisions (Morelli and Cohen, 2005). Oocytes and spermatocytes both contribute significantly to the development of the embryo, but oocytes are much larger than spermatocytes in size (Alberts et al. 2002). Thus, there may be unknown mechanisms differentially governing meiosis in a sex-specific manner to produce the distinct gametes.

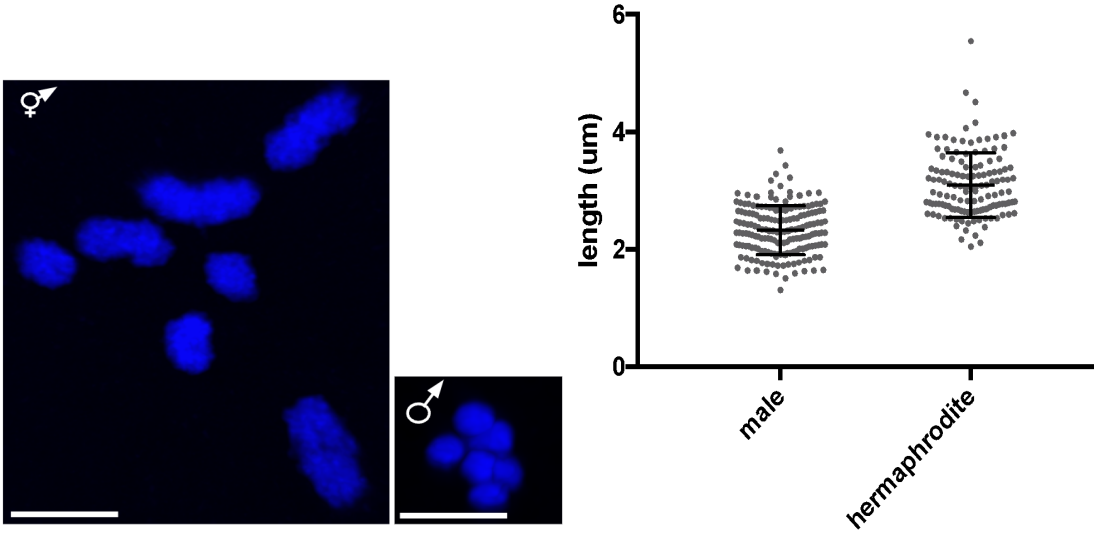

Figure 1.3: Bivalent Length is Smaller in *C. elegans* Male. Left: DAPI staining of chromosomes at diakinesis (blue) in spermatogenesis and oogenesis of wild-type hermaphrodites and males. Right: Chromosome bivalent length measured in both wild-type males and hermaphrodites. Scale bar = 2 μm.

To examine whether sex mechanisms contribute to the differences in meiotic chromosome structure, the difference in chromosome bivalent length between oogenesis and spermatogenesis in *C.elegans* was determined. The chromosome axial compaction of diakinesis chromosomes of hermaphrodites and male germ lines was measured using confocal microscopy with airyscan detector and Imaris imaging software. We found a significant difference in diakinesis bivalent length between oocytes and spermatocytes (Lauren Salvitti unpublished data). Hermaphrodite diakinesis bivalents are significantly larger than that of males (average hermaphrodite bivalent length: 3.1µm; average male bivalent length: 2.3µm; $p < 0.001$) (**Figure 1.3**). This suggests that sex-specific mechanisms might contribute to the distinct chromosomal compaction in between hermaphrodites and males. To examine this further, Dr. Lauren Salvitti, a previous postdoctoral researcher of the Jaramillo-Lambert Lab, analyzed chromosome bivalent axial compaction of diakinetic chromosomes in wild-type versus mutants related to chromosome compaction and post-translational modifications of histones in both males and hermaphrodites at 20℃ (**Figure 1.4**). Bivalent length of *him-8(e1489)* (a mutation that causes sex chromosome nondisjunction for the production of males)*, htas-1(ok1573)* (sperm-specific histone H2A variants; see appendix) and *met-2(n4256)* were reduced compared to wild type and *set-25(n5021)* in spermatogenesis (N2: 2.86 µm, *him-8(e1489)*: 2.32 µm*, htas-1(ok1573)*: 2.61 µm*, met2(n4256)*: 2.53 µm, and *set-25(n5021)*: 2.74 µm). On the other hand, in oogenesis, the bivalent length of *htas-1(ok1573)* and *met-2(n4256)* were comparable to both wild type and *him-8(e1489),* while a reduction of bivalent length in oocytes was observed in *set-25(n5021)* (N2: 3.08 µm, *him-8(e1489)*: 2.92 µm ,

htas-1(ok1573): 3.08 µm*, met-2(n4256)*: 3.09 µm, and *set-25(n5021)*: 2.88 µm). The results of the bivalent length measurements in both oocytes and spermatocytes indicate that *met-2* and *set-25* candidate genes play differential roles in chromosomal compaction and structure depending on the sex of the germline, but how these genes mediate bivalent length and size in both sexes of *C. elegans* and the consequences of disrupting bivalent length/structure is unknown.

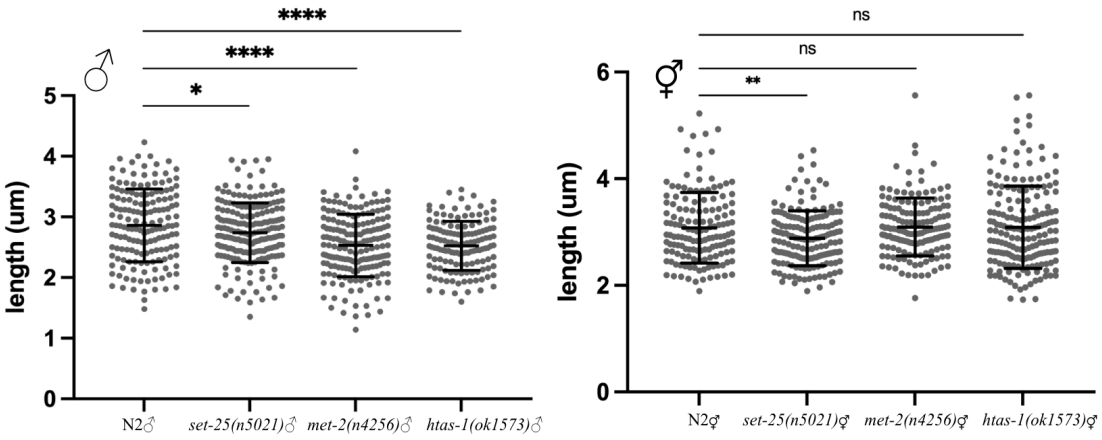

Figure 1.4 : Histone Post-translational Modifications Differentially Affect Oocyte and Spermatocyte Bivalent Length in *C. elegans*. Left: Bivalent length in spermatogenesis were measured in wild type, *htas-1(ok1573), met2(n4256)*, and *set-25(n5021)*. Bivalent length in spermatogenesis: n(N2) = 32, n[*set-25(n5021)*] = 37, n[*met-2(n4256)*] = 36, n[*htas-1(ok1573)*] = 28. Right: Bivalent length in oogenesis were measured in wild type, *htas-1(ok1573), met-2(n4256),* and *set-25(n5021)*. Bivalent length in oogenesis: n(N2) = 23, n[*set-25(n5021)*] = 27, n[*met-2(n4256)*] = 26, n[*htas-1(ok1573)*] = 29. Statistical analysis performed by unpaired t.test.. *p<0.05, **p<0.005, ****p<0.0001.

1.5 Proposed Hypothesis and Research Aims:

The main goal of this project was to determine the role of the histone methyltransferases on chromosome compaction and structure in oogenesis and spermatogenesis. My proposed hypothesis is that histone modifications (repressive histone modifications) mediated by the histone methyltransferases MET-2 and SET-25

have sexually dimorphic effects on chromosome structure and compaction. The first objective was to determine whether *met-2* and *set-25* induced changes in chromosome compaction have sex-specific impacts on fertility by performing embryonic viability assays and to determine the effects of the mutations on histone L9 methylation by examining the distribution of histone modifications (H3K9me2 and H3K9me3) between wild type and mutants through immunostaining of the these components in both oogenesis and spermatogenesis. The second objective was to determine if there is an epistatic or synthetic relationship between *met-2* and *set-25* in either oogenesis and spermatogenesis by examining the distribution of histone components in the germline and by measuring the axial compaction of the diakinesis bivalents of *met-2 set-25* double mutants in both spermatogenesis and oogenesis, and to investigate the impact of the double mutant on fertility via embryonic viability assays.

Chapter 2

MATERIALS AND METHODS

2.1 *C. elegans* Strains and Maintenance

Except where specified, all of the following strains were maintained at 20°C under standard conditions.

N2 (Bristol): wild-type isolate

CB1489: *him-8(el489)* IV

DG4915: *his-72(uge30)* III; *fog-2(oz40)* V

MT13293: *met-2(n4256)* III

MT17463: *set-25(n5021)* III

AJL52: *met-2(n4256)* III; *him-8(e1489)* IV

The following strain was maintained at 15°C under standard conditions.

GW638 *met-2(n4256) set-25(n5021)* III

2.2 Embryonic Viability Assays

A single L4 hermaphrodite of indicated genotype was placed onto MYOB plates spotted with OP50 *E. coli* at 20°C. Adult hermaphrodites were transferred onto a new plate every 24 hours. Worm transfers were repeated twice under the same temperature. The adult worms were discarded after three 24 hour periods. The number of live progeny and dead embryos of each plate were counted 24 hours after the adult worms were removed, and viability and brood size of each strain were calculated. Three or more independent trials were performed for each strain.

For embryonic viability mating assays (EVA), individual L4 hermaphrodites and six L4-young adult males of indicated genotype were placed on MYOB plates spotted with OP50 *E. coli* at 20°C and allowed to mate. The remaining steps of the EVA were repeated as above.

2.3 Immunostaining and DAPI Staining

Hermaphrodite and male ages were synchronized by picking worms at L4 stage and incubating at 20°C for 15 to 24 hours. Gonads of adult worms were dissected in 30 µl of 1x Egg buffer (118 mM NaCl, 48 mM KCl, 2 mM CaCl2 · 2H2O, 2 mM MgCl2 · 6H2O, 25 mM, HEPES, pH 7.4) and 0.1% Tween 20 on a glass coverslip. Following the dissection, 15 µl of the liquid was removed, and 15 µl 2% paraformaldehyde solution (16% paraformaldehyde from EM Sciences in 1x Egg buffer, 0.1% Tween 20) was added to the coverslip. 15 µl of the liquid was removed and discarded. A Superfrost Plus microscope slide was placed on the top of the coverslip containing dissected gonads, and the slide was flipped rightside up. The gonad tissue was allowed to fix for 5 min before placing the slide into liquid nitrogen. Once frozen, the coverslip was quickly removed, and the slide was immediately placed in - 20°C methanol for 1 min. The slide was then washed three times in PBST (1x PBS, 0.1% Tween 20) for 5 min. After the washes, the slide was placed in 0.7% BSA in PBST, a blocking solution, for 1 hour. 50 µl of primary antibody diluted in 0.7% BSA in PBST was added on the top of the dissected gonads. The slide was covered with a parafilm coverslip and incubated overnight (15 to 24 hours) in a humidified and dark chamber at room temperature. After the primary antibody incubation, the slide was washed 3 times in

PBST for 10 mins and incubated with 50 µl of secondary antibody diluted in 0.7% BSA in PBST in a humidified and dark chamber for 2 hours. The slide was washed 3 times in PBST for 10 mins in the dark, and it was then stained with 40 µl of DAPI (2 µg/mL) for 5 min. A final wash in PBST for 5 min was performed and the slide mounted on a coverslip with 8 µl of Vectashield. The edges of the coverslip were sealed with nail polish. Primary antibodies utilized in this study were: mouse H3K9me2 from Abcam [ab1220 lot # GR3377057-5 (1:500)]; rabbit H3K9me3 from Abcam [ab8898 lot # GR3414325-1 (1:500)]; rabbit anti-RNA polymerase II CTD repeat Ser2 from Abcam [ab5095 lot #GR3424202-1].

For DAPI staining, adult worms underwent gonad dissection and tissue fixation as above. The slide was then frozen in the liquid nitrogen. Once the slide was frozen, the coverslip was quickly removed from the slide, and it was immediately fixed in the -20°C methanol. After the methanol fixation, the slide was washed 3 times in PBST for 5 min, and 40 µl of DAPI (2 µg/mL) was added to the sample for 5 min. The slide final was washed in PBST for 5 min and mounted by adding 8 µl of Vectashield with the coverslip of the top. The edges of the coverslip were sealed by nail polish.

2.4 Image Collection, Processing and Measurement

Z-stack images of dissected gonads were obtained by using a Zeiss LSM880 confocal microscope. For each gonad sample, a full range of focal planes were selected to include the complete gonad, with a constant Z-step of 0.2 µm. Image processing was performed using Fiji is Just ImageJ. The range of focal planes used for z-stack projections in figures was chosen depending on the image and whether the image was

of a male or a hermaphrodite gonad. Adobe Photoshop was utilized to merge channels and adjust the resolution of each image as well as the brightness and contrast for better visualization.

Bivalent length measurement was done using Huygens Professional 20.10 software (SVI) and Imaris Cell Imaging software (Thermo Fisher Scientific). Z-stack Images for bivalent length measurements were deconvolved by using Huygens. The deconvolved images were visualized and the measurements of the length of individual diakinesis bivalents were completed using Imaris. The bivalent length data of each strain were entered in a spreadsheet and were plotted using Prism.

Chapter 3

RESULTS

3.1 Loss of MET-2 and SET-25 does not affect progeny viability

Histone methyltransferases were previously discovered to differentially affect the bivalent length in both oogenesis and spermatogenesis. Diakinesis bivalent length of spermatocytes are reduced in *met-2(n4256),* while diakinesis bivalent length is decreased in *set-25(n5021)* oocytes (Salvitti, L. unpublished data). To determine whether the changes in bivalent length of the mutants affect embryonic viability, embryonic viability assays (EVA) were first performed on self-fertilizing hermaphrodites of N2 (wild type), *met-2(n4256)*, and *set-25(n5021)* at 20℃. Embryonic viability of *met-2(n4256)* was slightly, but significantly reduced compared to wild type [*met-2(n4256)* is 88.3% vs. N2 is 98.4%, $p < 0.0001$, (**Figure 3.1**)]. However, the percent embryonic viability of *set-25(n5021)* progeny was not significantly different from wild type [*set-25(n5021)* is 98.3% vs. N2 is 98.4%, $p = 0.9205$, (**Figure 3.1**)]. In addition, I also observed a significant reduction in the average brood size of *met-2(n4256)* self-fertilizing hermaphrodites compared to those of wild type and *set-25(n5021)* [N2 is 271.3; *set-25(n5021)* is 275.8; *met-2(n4256)* is 161.7 (**Figure 3.2**)]. Interestingly, the results of the *met-2(n4256)* embryonic viability assays were highly variable. Some of the *met-2(n4256)* hermaphrodites laid no progeny and were sterile while some showed wild type fertility resulting in a large standard deviation (**Figure 3.2**). The reduction of embryonic viability and brood size of *met-2(n4256)* hermaphrodites suggests that changes to bivalent length may have consequences on the quality of oocytes or spermatocytes.

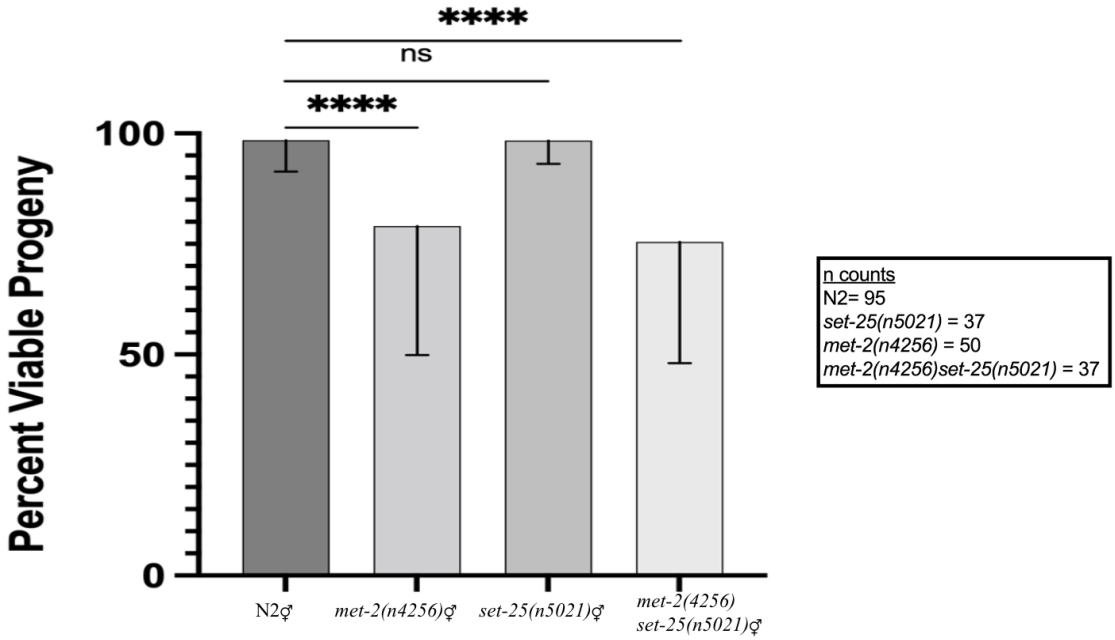

Figure 3.1: *met-2(n4256)* reduces the embryonic viability in hermaphrodites. Embryonic viability assays were performed to calculate the percentage of the embryonic viability of hermaphrodites self mating in wild type, *met-2(n4256), set-25(n5021)* and *met-2(n4256) set-25(n5021)* at 20℃. Error bar represents the standard deviation of the average percent of embryonic viability. Statistical analysis performed by unpaired t.test. ****p<0.0001.

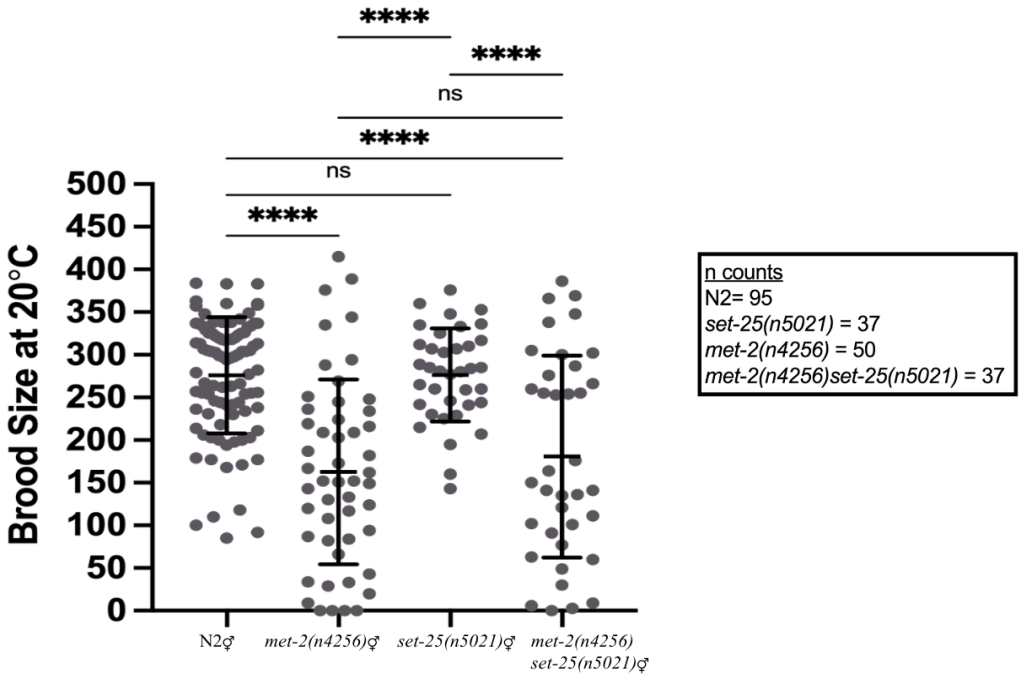

Figure 3.2: *met-2(n4256)* reduces the brood size in hermaphrodites. Brood size of hermaphrodites self mating was counted in WT, *met-2(n4256), set-25(n5021)* and *met-2(n4256)set-25(n5021)* at 20℃. Statistical analysis performed by one-way ANOVA. ****p<0.0001.

To determine if the reduced embryonic viability and decreased brood size of *met-2(n4256)* is caused by a defect in oogenesis, I crossed *met-2(n4256)* mutant hermaphrodites with wild-type males (N2) and embryonic viability of cross progeny was determined. At the same time, *set-25(n5021)* hermaphrodites were also crossed with wild-type males. The percent embryonic viability of *met-2(n4256)* was restored to wild-type levels (95.6%) after mating with N2 males. The percent embryonic viability of *set-25(n5021)* was not changed from hermaphrodite self mating (**Figure 3.3)**. These data suggest that the decrease in embryonic viability observed in *met-2(n4256)* is not due to an oogenesis defect alone. To determine if *met-2(n4256)* [*set-25(n5021)* was also tested] has a sperm-specific defect, *met-2(n4256); him-8(e1489)* males were mated to *fog-2(oz40)* females. We crossed *met-2(n4256)* with *him-8(e1489)* to create *met-2(n4256); him-8(e1489)*. The mutant *him-8(e1489)* strain produces ~40% male self-progeny through X-chromosome nondisjunction (Phillips et al., 2005). *fog-2(oz40)* females contain a mutation in the germline sex determination pathway that results in the failure of *fog-2(oz40)* animals to produce sperm (Schedl and Kimble, 1988), so *fog-2(oz40)* XX animals are essentially females. Control males (N2) crossed with *fog-2(oz40)* females produced progeny with a high percentage of embryonic viability (99.0%). Both *met-2(n4256); him-8(e1489)* and *set-25(n5021)* males also produced viable cross progeny [99.0% and 99.3% respectively (**Figure 3.4**)]. T-test comparison of embryonic viability of *met-2(n4256); him-8(e1489)* mutant males is not significantly different from wild type male crosses (N = 99.0%). In addition, the embryonic viability

of *set-25(n5021)* males crossed with *fog-2(oz40)* females shows no significant difference compared to wild type male crossed with *fog-2(oz40)* at 24℃ (**Figure 3.5**). Together, these data indicate that the change in diakinesis chromosome length of *set-25(n5021)* oocytes does not affect the production of oocytes nor spermatocytes. The change in diakinesis chromosome length of *met-2(n4256)* spermatocytes is associated with a decrease in embryonic viability and brood size, however, the embryonic viability defect does not appear to be either sperm or oocyte specific.

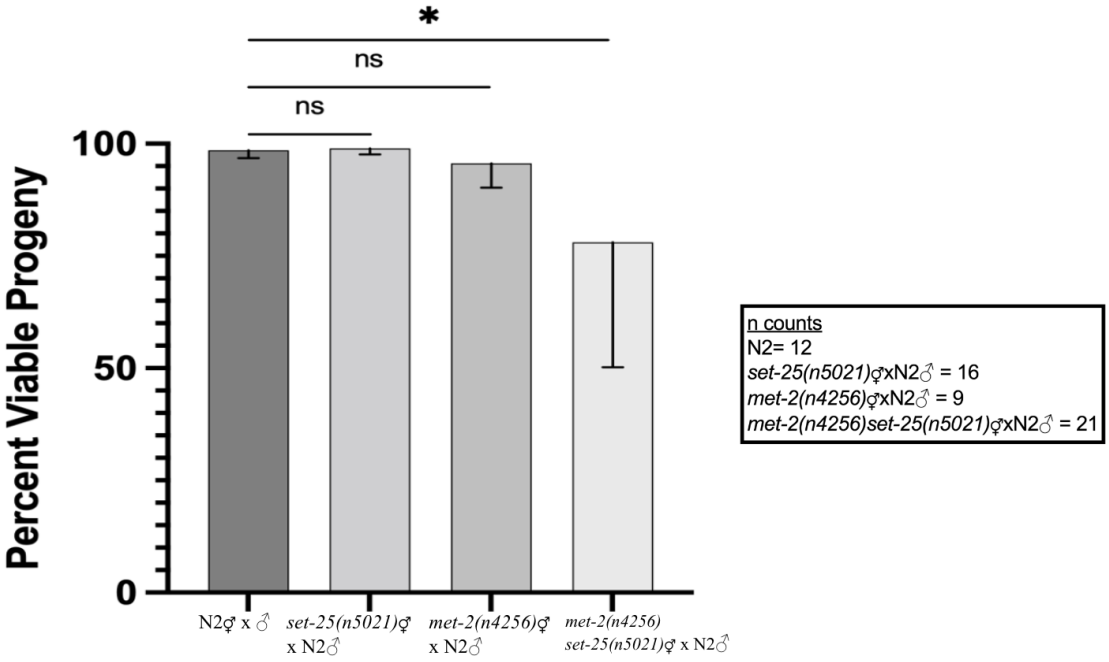

Figure 3.3: Embryonic viability of *met-2(n4256)* hermaphrodites is rescued by mating to wild-type males. Embryonic viability assays were performed to calculate the percentage of embryonic viability of N2 (wild type)♀ x ♂, *met-2(n4256)*♀ x N2♂, *set-25(n5021)*♀ x N2 ♂, and *met-2(n4256) set-25(n5021)*♀ x N2♂ at 20℃. Error bar represents the standard deviation of the average percent of embryonic viability. Statistical analysis performed by unpaired t.test. *p<0.05.

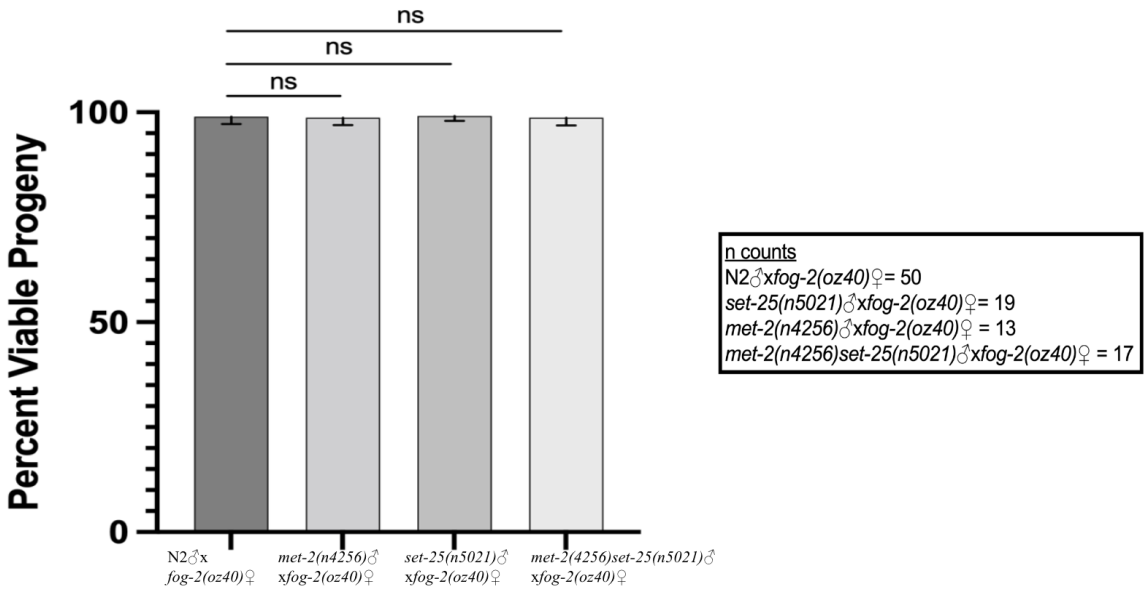

Figure 3.4: Loss of both MET-2 and SET-25 in spermatogenesis does not affect embryonic viability at 20℃. Embryonic viability assays were performed to calculate the average percent embryonic viability of N2 (wild type)♂ x *fog-2*♀, *met-2(n4256)*♂ x *fog-2*♀, *set-25(n5021)*♂ x *fog-2*♀, and *met-2(n4256) set-25(n5021)*♂ x *fog-2*♀ at 20℃. Error bar represents the standard deviation of the average percent of embryonic viability. Statistical analysis performed by unpaired t.test.

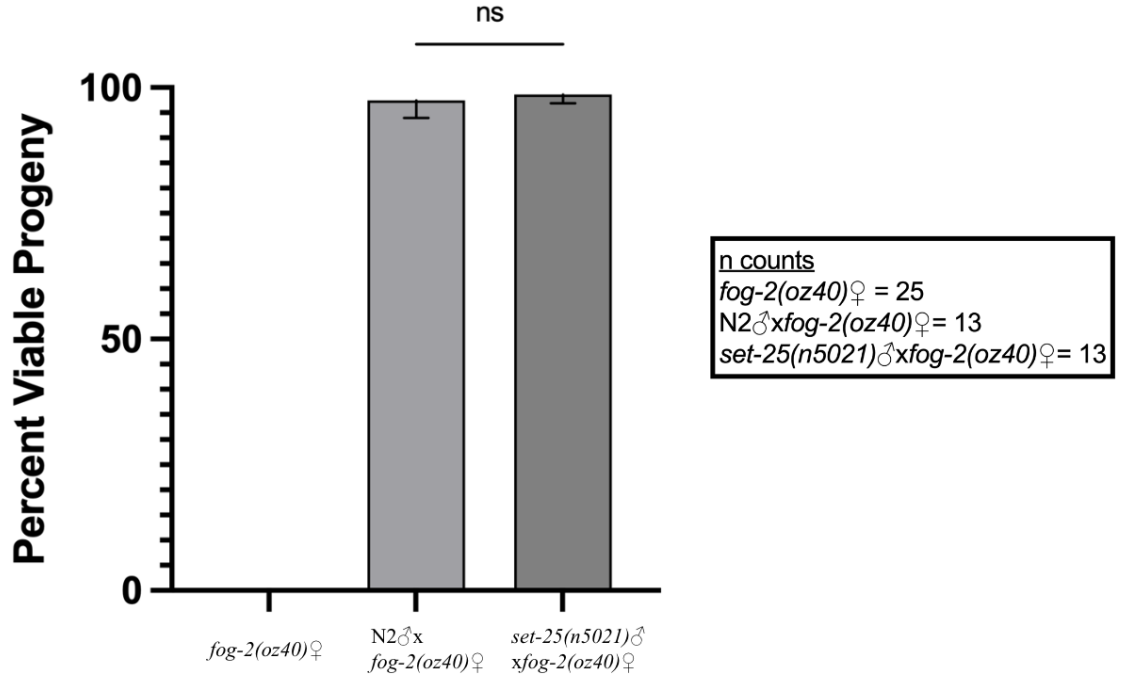

Figure 3.5: Loss of SET-25 Has no Effect on embryonic viability in spermatogenesis at 24℃. Embryonic viability assays were performed to calculate the average percent of embryonic viability of WT♂ x *fog-2*♀ and *set-25(n5021)*♂ x *fog-2*♀

at 24℃. Error bar represents the standard deviation of the average percent of embryonic viability. Statistical analysis performed by unpaired t.test.

3.2 The combined loss of both MET-2 and SET-25 results in an increase of chromosome bivalent length in spermatogenesis and oogenesis

It was previously suggested that MET-2 and SET-25 work in a stepwise manner in histone methylation (Towbin et al., 2012). Although, we found that either the loss of MET-2 or SET-25 have differential impacts on the diakinesis bivalent length in spermatogenesis and oogenesis, loss of both enzymes might also affect chromosome compaction in gametogenesis of both sexes. To determine if the loss of both MET-2 and SET-25 together can alter the diakinesis bivalent length in oogenesis and spermatogenesis, I measured diakinesis bivalent length of *met-2(n4256) set-25(n5021)* double mutants and compared them to the average bivalent lengths of wild type and both single mutants. Surprisingly, we found that the diakinesis bivalent length of the *met-2(n4256) set-25(n5021)* double mutant was significantly increased in both oogenesis and spermatogenesis (Oocyte: N2 = 3.08 μm, *met-2(n4256)* = 3.09 μm, *set-25(n5021)* = 2.88 μm, *met-2(n4256) set-25(n5021)* = 4.55 μm; Spermatocyte: N2 = 2.86 μm, *met-2(n4256)* = 2.53 μm, *set-25(n5021)* = 2.74 μm, *met-2(n4256) set-25(n5021)* = 3.65 μm) (**Figure 3.6**). From the differential reduction of diakinetic bivalent length in single mutants and dramatic elongated bivalent in absence of both HMTs, I conclude MET-2 and SET-25 are required for the regulation of the diakinesis chromosome compaction in oogenesis and spermatogenesis.

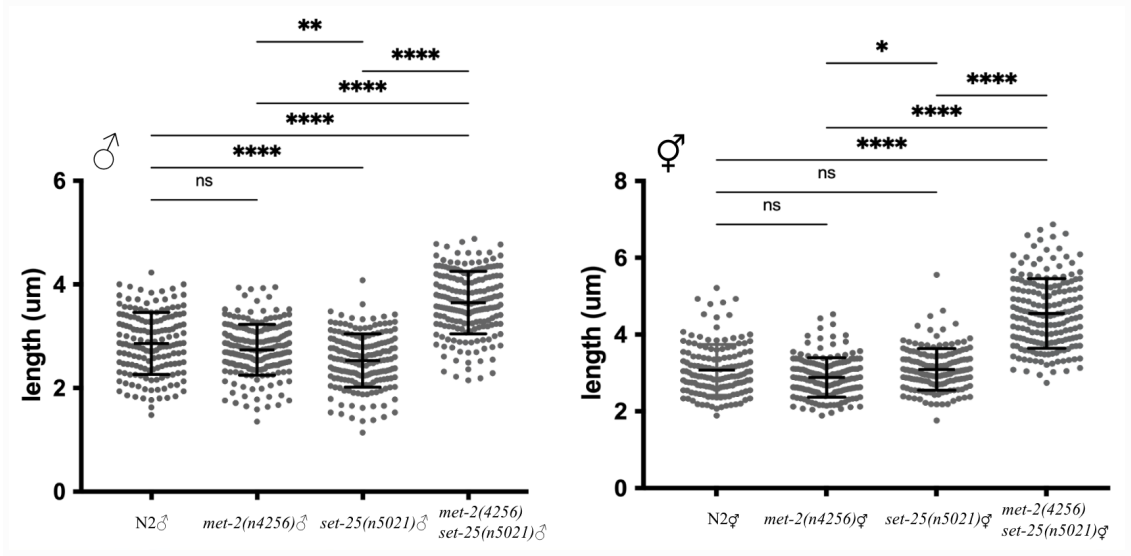

Figure 3.6: *met-2(n4256) set-25(n5021)* Bivalent Length Increases in Both Oogenesis and Spermatogenesis. The bivalent lengths of chromosomes from the double mutant *met-2(n4256) set-25(n5021)* were measured in both spermatogenesis and oogenesis. Bivalent length is increased in both oocytes and spermatocytes. Bivalent length in spermatogenesis: n(N2) = 32, n[*set-25(n5021)*] = 37, n[*met-2(n4256)*] = 36, n[*met-2(n4256)set-25(n5021)*] = 39. Bivalent length in oogenesis: n(N2) = 23, n[*set-25(n5021)*] = 27, n[*met-2(n4256)*] = 26, n[*met-2(n4256)set-25(n5021)*] = 32. Statistical analysis performed by one-way ANOVA. *p<0.05, **p<0.005, ****p<0.0001.

3.3 Loss of both MET-2 and SET-25 does not affect progeny viability

To further investigate whether the increase in diakinesis bivalent length has an impact on progeny viability in both oogenesis and spermatogenesis, I conducted embryonic viability assays for the *met-2(n4256) set-25(n5021)* double mutant hermaphrodites and males at 20℃. In self-fertilizing hermaphrodites the percent progeny viability of the double mutant is reduced (84%) compared to that of wild type (98.4%), and the student t-test result indicates that the slight reduction is significantly different from wild type ($p < 0.0001$) (**Figure 3.1**). The brood size of the *met-2(n4256) set-25(n5021)* double mutant was significantly reduced compared to wild type [*met-2(n4256) set-25(n5021)* = 174.7 vs. N2 = 271.3, $p < 0.0001$, **Figure 3.2**). The

pattern of brood viability for *met-2(n4256) set-25(n5021)* was similar to *met-2(n4256)* where some of the hermaphrodites did not produce offspring and were sterile (**Figure 3.2**). Mating assays revealed that the viability of progeny from *met-2(n4256) set-25(n5021)* hermaphrodites crossed with N2 (wild type) males was significantly reduced (*met-2(n4256) set-25(n5021)* is 86.1%, N2 is 98.3%, p = 0.0164) compared to those of N2 mating with single mutant hermaphrodites (**Figure 3.3**). On the other hand, the reciprocal cross, *met-2(n4256) set-25(n5021)* males crossed with *fog-2(oz40)* females, had an average percent progeny viability of 99.1%, which is comparable to the wild type males mated with *fog-2(oz40)* females (99.0%) (**Figure 3.4**). From these results, the increase in diakinesis bivalent length in *met-2(n4256) set-25(n5021)* double mutants appears to have a larger impact on the quality of oocytes than spermatocytes

3.4 H3K9me2 does not localize on diakinesis chromosomes in the germlines of males and hermaphrodites

Previous studies found that H3K9me2 is found throughout the germline of wild type *C. elegans* hermaphrodites undergoing oogenesis and is particularly concentrated on the subset chromosomes found in late prophase. Bessler et al., 2010 previously reported that the localization of H3K9me2 at diakinesis starts to diminish but is still detectable in diakinesis. To confirm H3K9me2 localization at diakinesis in both wild type and mutants, I performed immunostaining of H3K9me2 in wild type (N2) hermaphrodite vs *met-2(n4256)* hermaphrodite germlines. Image analysis shows that H3K9me2 was not detectable at diakinesis of wild type nor *met-2(n4256)* hermaphrodite germlines. Immunostaining against H3K9me2 was also conducted on control [*him-8(e1489)*] males and *met-2(4256); him-8(e1489)* mutant males (**Figure**

3.7). Similar to oogenesis, the localization of H3K9me2 was undetectable at diakinesis of both *him-8(e1489)* males and *met-2(4256); him-8(e1489)* mutant males (**Figure 3.7**). As Histone H3 lysine 9 dimethylation was not detected on diakinetic nuclei of both oogenesis and spermatogenesis in either wild-type or mutant germlines, it is unclear how these histone methyltransferases are influencing chromosome structure at this stage of meiotic prophase I.

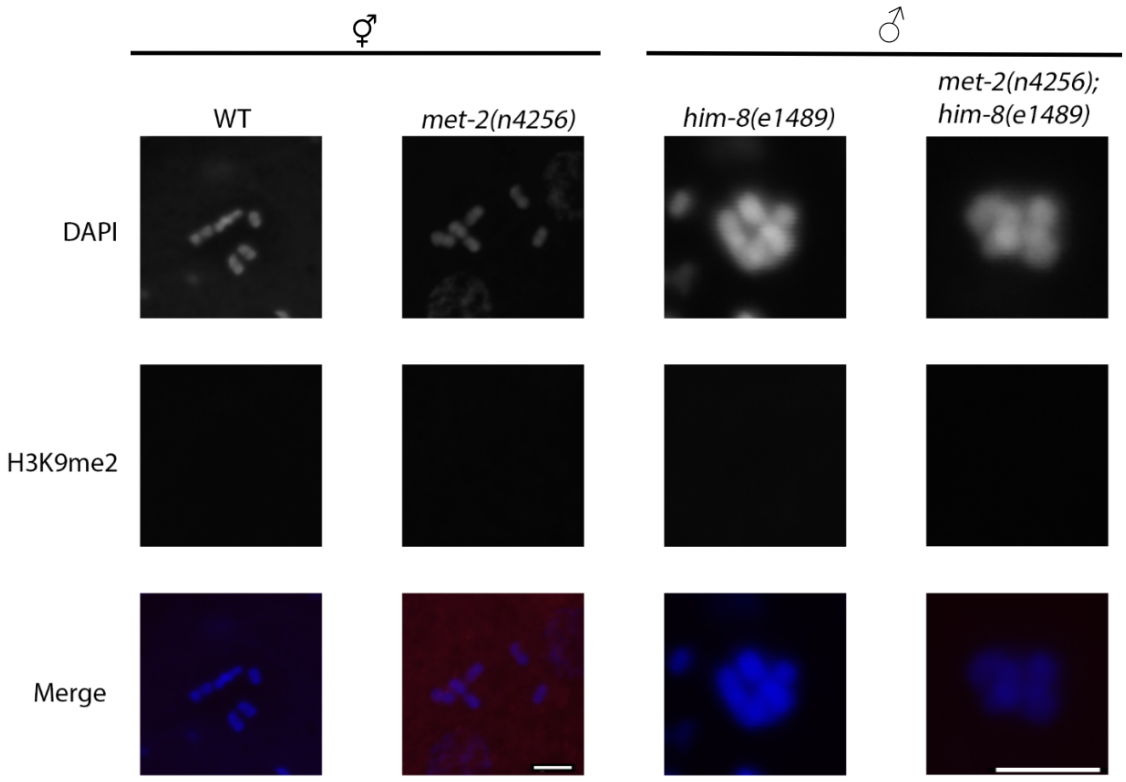

Figure 3.7: H3K9me2 is not detectable on chromosomes within diakinesis nuclei of all strains. Germline diakinesis nuclei of wild type and *met-2(n4256)* hermaphrodites stained with H3K9me2 in red (middle panels) and DAPI in blue (top panels) shown in the left two columns; Germline diakinesis nuclei of wild type and *met-2(n4256)* males stained with H3K9me2 in red (middle panels) and DAPI in blue (top panels) shown in the right two columns. Scale bar = 5 μm.

3.5 Loss of MET-2 does not affect the conversion of H3K9me3 at diakinesis

Unlike H3K9me2, H3K9me3 was previously discovered to be broadly distributed throughout the germline of wild type hermaphrodite germlines, and strongly

localized on all the chromosomes at diakinesis (Bessler et al., 2010). To examine the localization of H3K9me3 at diakinesis of oogenesis and spermatogenesis immunostaining of H3K9me3 and image analysis were conducted on germlines from N2 hermaphrodites, *met-2(n4256)* hermaphrodites, *him-8(e1489)* males, and *met-2(4256); him-8(e1489)* males. During the image analysis, H3K9me3 was detected within diakinetic nuclei of wild type and *met-2(n4256)* hermaphrodites during oogenesis and in control *him-8(e1489)* and *met-2(4256); him-8(e1489)* males during spermatogenesis **(Figure 3.8)**. These results suggest that the loss of MET-2 and its mediated H3K9 dimethylation has no effect on H3K9 trimethylation at diakinesis.

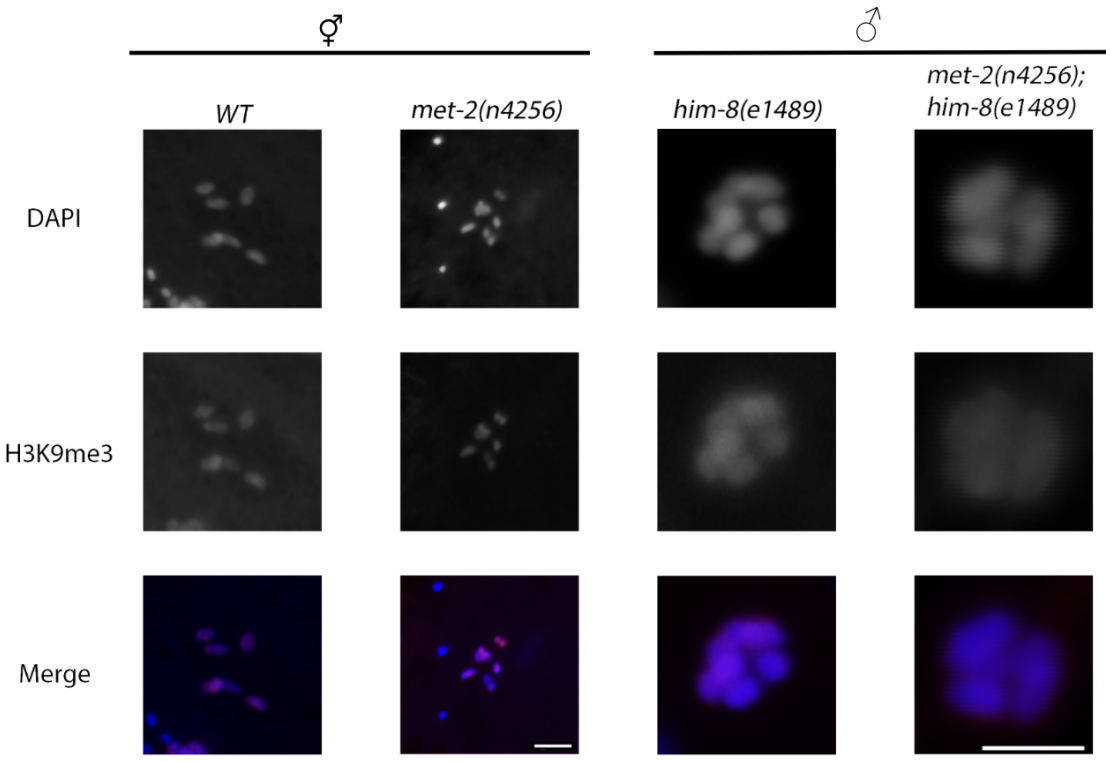

Figure 3.8: H3K9me3 is strongly detected on all the chromosomes of diakinesis nuclei in both oogenesis and spermatogenesis. Germline diakinesis nuclei of wild type and *met-2(n4256)* hermaphrodites stained with H3K9me3 in red (middle panels) and DAPI in blue (top panels) shown in the left two columns; Germline diakinesis nuclei of wild type and *met-2(n4256)* males stained with H3K9me3 in red (middle panels) and DAPI in blue (top panels) shown in the right two columns. Scale bar = 5 μm.

3.6 The switch off of global transcription is delayed in *met-2(n4256)* spermatogenesis

Global transcription during *C. elegans* male spermatogenesis was previously found to abruptly turn off as the chromosomes transition into the karyosome stage in N2 (wild type) male gonads labeled with an antibody against the phosphorylated c-terminal domain of RNA polymerase II (Kostrouchova et al., 1998; Ragal et al., 2020; Shakes et al., 2009). I next asked whether the *met-2(n4256)* induced reduction in the bivalent length (more compact) of spermatocytes caused a change in global transcription. To address this question immunostaining against active RNA polymerase II was performed on *met-2(n4256)* and control [*him-8(e1489)*] male germlines and the localization pattern examined by confocal microscopy. High intensity localization of active RNA polymerase II was observed at the diplotene region with an abrupt decrease in karyosome nuclei in control male germlines consistent with the results of Ragle et al., 2020 (**Figure 3.9**). In *met-2(n4256)* male germlines active RNA polymerase II was observed at the diplotene region, however, active RNA polymerase II gradually decreased and localization extended into the karyosome region. These results indicate that loss of *met-2* and changes in chromosome compaction during spermatogenesis have consequences on global gene transcription.

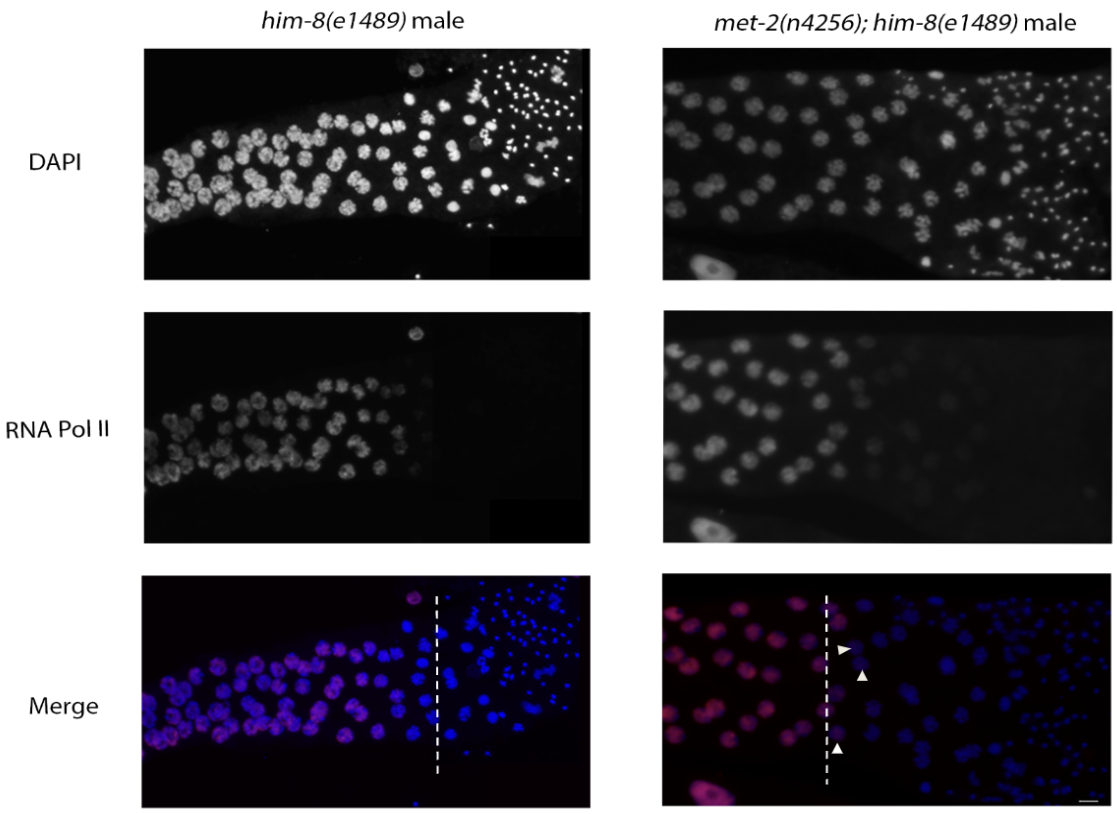

Figure 3.9: Delayed Switch off of Global Transcription in *met-2(n4256)* Mutant Male. Control wild type [*him-8(e1489)*] and *met-2(n4256)* mutant male gonads co-labeled with RNA pol II (red) and DAPI (blue) in the condensation zone. Scale bar = 5 μm.

Chapter 4

DISCUSSION

In this research project, I have observed the effects of two histone methyltransferase proteins, MET-2 and SET-25, on diakinetic chromosome compaction and structure. Previous data from our lab found that the *set-25(n5021)* mutation results in reduction of diakinetic bivalent length in oocytes; contrariwise, loss of MET-2 [*met-2(n4256)*] causes a decrease in bivalent length of diakinetic spermatocytes (Salvitti, L. unpublished data). Interestingly, I have found that the loss of both MET-2 and SET-25 results in elongated bivalent lengths in both spermatogenesis and oogenesis. Embryonic viability results demonstrate that *set-25(n5021)* does not significantly impact the embryonic viability of progeny from homozygous mutant animals. However, both embryonic viability and the brood size of *met-2(n4256)* hermaphrodites was reduced. Immunostaining against H3K9me2 is undetectable in both wild type and *met-2(n4256)* hermaphrodites at diakinesis of oogenesis and a similar localization pattern was shown in both control [*him-8(e1489)*] males as well as *met-2(4256); him-8(e1489)* mutant males. Trimethylation of histone H3 lysine 9 localized on the diakinetic bivalents of control and mutant hermaphrodites and males. Lastly, I found that loss of *met-2* disrupts the turning off of global transcription.

4.1 Defects in chromosomal structure and compaction in MET-2 and SET-25 mutants

Methylation of H3K4, H3K36, and H3K79 are primarily correlated with transcriptional activation and association with euchromatin, in contrast, methylation of H3K9, H3K27, and H4K20 are the marks for silencing gene expression and favorable

for heterochromatin (Bessler et al., 2010; Peters et al., 200; Fischle et al., 2003). Previous studies demonstrated that promoters are co-enriched for the repressive histone modification histone H3 lysine 27 trimethylation and for the activating histone H3 lysine 4 trimethylation in embryonic stem cells, yet there is no evidence for the association between histone H3 lysine 9 methylation and the promotor at embryonic stages (Dunican et al., 2020; Bernstein et al., 2006; Harikumar and Meshorer, 2015).

Homologous chromosomes condense in late meiotic prophase I (diplotene and diakinesis), and chromosomes can be reorganized through post-translational modifications (PTMs) of histones. To better understand the differences in chromosome compaction between oogenesis and spermatogenesis a previous post-doctoral research assistant, Dr. Lauren Salvitti, measured diakinetic bivalent length in both oogenesis and spermatogenesis of wild type and loss-of-function mutants of a few candidate genes, which are primarilyy known for contributing to chromosomal structure and compaction. Her data showed that the diakinetic bivalent length of *set-25(n5021)* shortens in oogenesis, yet spermatocyte bivalent was reduced in *met-2(n4256)* (**Figure 1.4**). Recently, the Michael laboratory at the University of Southern California, posted a manuscript on BioRxiv (bioRxiv prepint doi: https://doi.org/10.1101/2022.08.28.505591, Belew et al., 2022) reporting similar experiments to what I have done. Belew et al., reported that reduction of either *met-2* or *set-25* function resulted in an increase in diakinesis bivalent length in oogenesis (spermatogenesis was not examined). These results are opposite of what I observed. Several differences in experimental methods may account for the discrepancy. First, Belew et al., used RNAi to knockdown *met-2* and *set-25* gene expression whereas I

used deletion mutants that result in null phenotypes. RNAi-mediated gene knockdown can be variable and no data was presented to indicate the degree to which gene expression of these two genes were depleted. The differences in phenotypes could be due to hypomorphic versus null versions of *met-2* and *set-25*. A second difference arises from the imaging approaches our two labs used. My bivalent measurements were performed on fixed chromosomes that were stained with DAPI and the images analyzed using advanced imaging software (Imaris). Bivalent length was then measured from 3D reconstructions of each chromosome. Belew et al., 2022 performed their imaging on live samples expressing histone tagged with mCherry and analyzed their images using ImageJ. Their measurements were taken from a single imaging plane and measured with the ImageJ line tool and reported as arbitrary units. Thirdly, only -2 oocytes (second to the most proximal oocyte) were used for bivalent measurements in Belew et al., 2022. For our experiments bivalent length was measured in the -1, -2, and -3 oocytes and is reported as an average across all chromosomes in the three most proximal oocytes. Chromosome compaction increases as the oocytes mature and approach the spermatheca, therefore, my measurements include chromosomes that could be more compact than those measured in Belew et al., 2022. Lastly, the Belew et al., 2022 manuscript has a much lower sample number than my study (15-20 vs. >50). Due to these differences, we believe that my study is more rigorous and may represent a more accurate picture than what was reported by Belew et al.

Histone H3 lysine 9 dimethylation (H3K9me2) and histone H3 lysine 9 trimethylation (H3K9me3) involves repression of gene expression (Peters et al., 2003). The absence of H3K9me2 signal in *met-2(n4256)* mutants indicates that the histone

methyltransferase MET-2 is required for H3K9me2 in *C. elegans* adult germlines (Bessler et al., 2010). The absence of H3K9me3 in *set-25(n5021)* deletion mutants indicates that SET-25 is a HMTs responsible for H3K9me3 (Towbin et al., 2012). The mechanism of the effects of MET-2 mediated H3K9me2 and SET-25 mediated H3K9me3 on diakinetic chromosome structure and compaction at gametogenesis remain unclear. Nevertheless, the presence of H3K9 methylation enhances the compaction of chromosomal arms through independent anchoring with the assistance of anchor protein CEC-4 (Bian et al., 2020). Our results demonstrate that the bivalent length of both oocytes and spermatocytes of the *met-2(n4256) set-25(n5021)* double mutant are elongated at diakinesis (**Figure 3.6**). This might suggest that either MET-2 or SET-25 mediated methylations on H3K9 are essential for the diakinetic chromosome compaction in oogenesis and spermatogenesis and that the loss of both disrupts this process. It is possible that these histone methyltransferases, MET-2 and SET-25, act in a compensatory role when one is absent due to the distinct changes of bivalent length in single mutants compared to the double mutant line. qRT-PCR is one method that can be used to measure the abundance of the transcript of one HMT when the other is absent. This would help clarify if compensation happens when either MET-2 or SET-25 is absent. As we only measured the bivalent length of homozygous *met-2(n4256) set-25(n5021)* double mutants, the analysis of chromosome compaction and structure should be done on heterozygous *met-2(n4256) set-25(n5021)*mutants to examine if it could rescue the elongated bivalent length in both oocytes and spermatocytes that is observed in the homozygous double mutant.

4.2 Histone methyltransferase MET-2 is essential for embryonic performance

To investigate the relationship between bivalent length and embryonic performance, I characterized the embryonic viability in mutants of the histone methyltransferase genes and compared the findings to that of wild type at 20°C. Embryonic viability of *met-2(n4256)* hermaphrodite selfing is reduced, but restored by mating with wild type N2 males (**Figure 3.1 and Figure 3.2**). On the other hand *set-25(n5021)* and *met-2(n4256) set-25(n5021)* double mutant embryonic viabilities of hermaphrodites is comparable to that of wild type; however, there is a significant difference between wild type and *met-2(n4256) set-25(n5021)* in mating with N2 males with decrease in cross progeny (**Figure 3.1 and Figure 3.2**). In contrast, embryonic viabilities of *met-2(n4256), set-25(n5021) and met-2(n4256) set-25(n5021)* double mutant males crossed with *fog-2(oz40)* female does not incur a significant reduction (**Figure 3.4**). Recovery of embryonic viability by introduction of wild type sperm in *met-2(n4256)* suggests that spermatocytes of *met-2(n4256)* hermaphrodite are defective, but *met-2(n4256)* males mated with wild type females did not result in embryonic lethality, thus the cause of the *met-2(n4256)*-induced embryonic lethality remains unknown at this time. Interestingly, the brood size of *met-2(n4256)* hermaphrodite selfing is half that of wild type hermaphrodites (**Figure 3.2**). So, although sperm may not be the source of *met-2(n4256)*-induced embryonic lethality, *met-2* defective sperm may be the reason for the reduction in fecundity. Additional tests such as sperm activation assays and sperm transfer assays can determine if *met-2(n4256)* produce defective sperm. In has also been previously reported that *met-2(n4256)* requires longer timing of somatic development of synchronized larvae at

20°C, which indicates loss of MET-2 leads to stochastic delays in development (Padeken et al., 2019). This developmental delay in *met-2(n4256)* likely contributes to the reduction of brood size, but the mechanism is unsolved. The *met-2(n4256) set-25(n5021)* mutant, contrarily, shows germline lethality and stochastic delays in development (Padeken et al., 2019), and it is also characterized with elevated levels of transcripts from transposable elements, satellite sequences as well as inappropriately expressed pseudogenes and tissue-specific mRNAs (Zeller et al., 2016). As only homozygous *met-2(n4256) set-25(n5021)* mutants were used in the embryonic viability assays, embryonic viability assay should also be done on heterozygous *met-2(n4256) set-25(n5021)* double mutants to observe if its phenotype could rescue embryonic performance shown in homozygous *met-2(n4256) set-25(n5021)*.

4.3 Step-wise methylation of H3K9 may not be present in the *C. elegans* germline

It has been previously proposed that a stepwise relationship of histone H3 lysine 9 methylation is mediated by MET-2 and SET-25 in the nuclei of *C. elegans* embryos. In this model MET-2 is involved in the addition of histone H3 lysine 9 monomethylation (H3K9me1) and dimethylation (H3K9me2) in the cytoplasm, then SET-25 converts H3K9me2 to H3K9 trimethylation (H3K9me3) at the nuclear periphery (Towbin et al., 2012; Bian et al., 2020). In addition, previous studies revealed that the signal of mono-, di-, and trimethylation of H3K9 were all diminished in *met-2(n4256)* mutants (Towbin et al., 2012; Bessler et al., 2010; Andersen and Horvitz, 2007). Conversely, trimethylation was barely detectable, while mono- and

dimethylation shows wild type levels in *set-25* deletion mutants. In wild type hermaphrodites, low intensity of H3K9me2 and high intensity of H3K9me3 were detected in the adult hermaphrodite germline (Bessler et al., 2010). However in this study, H3K9me2 was not detected in the diakinesis region in either control or *met-2(n4256)* hermaphrodites and males (**Figure 3.7**). The paper previously showing H3K9me2 was published over 10 years ago and although the same antibody is still available, the lot number between then and now has changed. Bessler et al., 2010 did report that the H3k9me2 staining was faint at diakinesis and slight differences in the antibodies used may be why it is no longer detectable at diakinesis. Localization of H3K9 trimethylation was detected at high intensity on diakinesis chromosomes of both wild type and *met-2(4256)* oogenic and spermatogenic germlines (**Figure 3.8**). Similar results were also reported in the Belew et al., 2022 preprint. The presence of H3K9me3 in *met-2(n4256)* mutants suggests that SET-25 does not require the actions of MET-2 prior to H3K9me3 deposition in the *C. elegans* germline. This could be due to other undefined proteins or complexes that might also contribute to the deposition of H3K9me1/2 prior to the SET-25 mediated H3K9me3 conversion or that SET-25 can mediate the deposition of all three methyl groups.

4.4 MET-2 is important for the chromosome condensation at the karyosome in spermatocytes.

Unlike oogenesis, *C. elegans* spermatogenesis includes an extended stage after diplotene of meiotic prophase defined as the karyosome stage where chromosome aggregation happens (Shakes et al., 2009). My immunostaining results against RNA polymerase II demonstrates that global transcription was ceased before entering

karyosome in control male gonads, but delayed cessation of global transcription occurs in *met-2(n4256)* mutant males (**Figure 3.9**) (Kostrouchova et al., 1998; Ragle et al., 2020; Shakes et al., 2009). Belew et al., 2022 also observed the progression of global transcription and its switch off within the condensation zone in wild type and *met-2(n4256)* mutant males. RNA pol II signals were retained through the condensation zone in *met-2(n4256)* mutant germlines (Belew et al., 2022 preprint). These data indicate that loss of *met-2* function disrupts the regulation of gene transcription in spermatogenesis. Perhaps the expression of genes that should normally be turned off in late meiotic prophase are one of the causes contributing to the reduced brood size observed in *met-2(n4256)* and *met-2(n4256) set-25(n5021)* animals. Future studies should include analysis of global gene transcription in *set-25(n5021)* and *met-2(n4256) set-25(n5021)* males. Disruption of chromosome condensation at the karyosome might be a factor that contributes to spermatocyte defects when there is a loss of function in MET-2. It would be interesting to determine which genes have prolonged gene expression in *met-2(n4256)* mutant males. One approach could be RNAseq on wild type versus *met-2(n4256)* germlines to determine the genes with misregulated gene expression.

4.5 Conclusion

Histones play a crucial role in the regulation and organization of chromatin and gene expression through post-transcriptional modifications. I have characterized the impact of two histone methyltransferases, MET-2 and SET-25, on chromosome compaction and structure in spermatogenesis and oogenesis as well as associated

viability of progeny. Localization of H3K9me2 and H3K9me3 revealed MET-2 mediated H3K9me1/2 is not the only precursor of SET-25 regulated H3K9me3. I have also shown that a delay in global transcription occurs in loss of function *met-2* mutants. The mechanisms behind differential chromosome compaction in oogenesis and spermatogenesis and the connection between the chromosome compaction and embryonic performance remain unsolved. Future experiments to examine gene transcription and sperm quality will help bridge the connection between histone modifications and chromosome structure in spermatogenesis vs. oogenesis.

REFERENCES

Altun, Z.F., Herndon, L.A., Wolkow, C.A., Crocker, C., Lints, R. and Hall, D.H. (2002-2021). *Introduction to C. elegans Anatomy.* WormAtlas. https://www.wormatlas.org/hermaphrodite/introduction/IMAGES/introfig6leg.htm

Andersen, E. C., & Horvitz, H. R. (2007). Two C. elegans histone methyltransferases repress lin-3 EGF transcription to inhibit vulval development. *Development*, *134*(16), 2991–2999. https://doi.org/10.1242/dev.009373

Andux, S., & Ellis, R. E. (2008). Apoptosis maintains oocyte quality in aging Caenorhabditis elegans females. *PLoS Genetics*, *4*(12). https://doi.org/10.1371/journal.pgen.1000295

Azumi, Y., Liu, D., Zhao, D., Li, W., Wang, G., Hu, Y., & Ma, H. (2002). Homolog interaction during meiotic prophase I in Arabidopsis requires the SOLO DANCERS gene encoding a novel cyclin-like protein. *EMBO Journal*, *21*(12), 3081–3095. https://doi.org/10.1093/emboj/cdf285

Barrière A. and M. A. Félix, 2014 Isolation of C. elegans and related nematodes. WormBook ed. The C. elegans Research Community, WormBook, 1-19. doi: 10.1895/wormbook.1.115.2, http://www.wormbook.org

Bernstein, B. E., Mikkelsen, T. S., Xie, X., Kamal, M., Huebert, D. J., Cuff, J., Fry, B., Meissner, A., Wernig, M., Plath, K., Jaenisch, R., Wagschal, A., Feil, R., Schreiber, S. L., & Lander, E. S. (2006). A Bivalent Chromatin Structure Marks Key Developmental Genes in Embryonic Stem Cells. *Cell*, *125*(2), 315–326. https://doi.org/10.1016/j.cell.2006.02.041

Bessler, J. B., Andersen, E. C., & Villeneuve, A. M. (2010). Differential localization and independent acquisition of the H3K9me2 and H3K9me3 chromatin modifications in the Caenorhabditis elegans adult germ line. *PLoS Genetics*, *6*(1). https://doi.org/10.1371/journal.pgen.1000830

Bian, Q., Anderson, E. C., Yang, Q., & Meyer, B. J. (2020). Histone H3K9 methylation promotes formation of genome compartments in Caenorhabditis elegans via chromosome compaction and perinuclear anchoring CELL BIOLOGY. *PNAS*, *117*(21), 11459–11470. https://doi.org/10.1073/pnas.2002068117/-/DCSupplemental

Bowman, G. D., & Poirier, M. G. (2015). Post-translational modifications of histones that influence nucleosome dynamics. In *Chemical Reviews* (Vol. 115, Issue 6, pp. 2274–2295). American Chemical Society. https://doi.org/10.1021/cr500350x

Brooker, A. S., & Berkowitz, K. M. (2014). The roles of cohesins in mitosis, meiosis, and human health and disease. *Methods in Molecular Biology*, *1170*, 229–266. https://doi.org/10.1007/978-1-4939-0888-2_11

Cahoon, C. K., & Libuda, D. E. (2019). Leagues of their own: sexually dimorphic features of meiotic prophase I. In *Chromosoma* (Vol. 128, Issue 3, pp. 199–214). Springer Science and Business Media Deutschland GmbH. https://doi.org/10.1007/s00412-019-00692-x

Corsi, A. K., Wightman, B., & Chalfie, M. (2015). A transparent window into biology: A primer on Caenorhabditis elegans. *Genetics*, *200*(2), 387–407. https://doi.org/10.1534/genetics.115.176099

Cui, M., & Han, M. (2007). Roles of chromatin factors in C. elegans development. *WormBook. 1-16*. https://www.ncbi.nlm.nih.gov/books/NBK19740/

Dunican, D. S., Mjoseng, H. K., Duthie, L., Flyamer, I. M., Bickmore, W. A., & Meehan, R. R. (2020). Bivalent promoter hypermethylation in cancer is linked to the H327me3/H3K4me3 ratio in embryonic stem cells. *BMC Biology*, *18*(1). https://doi.org/10.1186/s12915-020-0752-3

Fielenbach, N., & Antebi, A. (2008). C. elegans dauer formation and the molecular basis of plasticity. In *Genes and Development* (Vol. 22, Issue 16, pp. 2149–2165). https://doi.org/10.1101/gad.1701508

Fischle, W., Wang, Y., and Allis, C.D. (2003a). Histone and chromatin Y. (2002). A complex with chromatin modifiers that occupies E2F- cross-talk. Curr. Opin. Cell Biol. 15, 172–183.

Forer, A., & Wilson, P. J. (2000). Evidence that kinetochore fibre microtubules shorten predominantly at the pole in anaphase flea-beetle spermatocytes. *Chromosome Research*, 8(2):151-63. https://doi.org/10.1023/A:1009298620707

Gao, A. W., uit de Bos, J., Sterken, M. G., Kammenga, J. E., Smith, R. L., & Houtkooper, R. H. (2018). Forward and reverse genetics approaches to uncover metabolic aging pathways in Caenorhabditis elegans. In *Biochimica et Biophysica Acta - Molecular Basis of Disease* (Vol. 1864, Issue 9, pp. 2697–2706). Elsevier B.V. https://doi.org/10.1016/j.bbadis.2017.09.006

Greer, E. L., & Shi, Y. (2012). Histone methylation: A dynamic mark in health, disease and inheritance. In *Nature Reviews Genetics* (Vol. 13, Issue 5, pp. 343–357). https://doi.org/10.1038/nrg3173

Grey, C., & de Massy B. (2021). Chromosome Organization in Early Meiotic Prophase. *Frontiers in Cell Development Biology*. 9:688878. https://doi.org/10.3389/fcell.2021.688878

Harikumar, A., & Meshorer, E. (2015). Chromatin remodeling and bivalent histone modifications in embryonic stem cells. *EMBO Reports*, *16*(12), 1609–1619. https://doi.org/10.15252/embr.201541011

Herbette, M., Robert, V., Bailly, A., Gely, L., Feil, R., Llères, D., & Palladino, F. (2020, May 30). Cooperation between *Caenorhabditis elegans* COMPASS and condensin in germline chromatinorganization. *BioRxiv*. bioRxiv. https://doi.org/10.1101/2020.05.26.115931

HFM Peters, A., Kubicek, S., Mechtler, K., O, R. J., AHA Derijck, A., Perez-Burgos, L., Kohlmaier, A., Opravil, S., Tachibana, M., Shinkai, Y., Turner, code, Martens, J. H., & Jenuwein, T. (2003). Partitioning and Plasticity of Repressive Histone Methylation States in Mammalian Chromatin modifying histone N termini and of chromatin-associ-ated proteins that specifically bind to selective histone modifications gave rise to the "histone code" hypothe-sis, proposing an epigenetic mechanism that may signif-icantly extend the information potential of the genetic. In *Molecular Cell* (Vol. 12). http://www.molecule.org/cgi/content/full/12/6/1577/DC1

Hirose, Y., Suzuki, R., Ohba, T., Hinohara, Y., Matsuhara, H., Yoshida, M., Itabashi, Y., Murakami, H., & Yamamoto, A. (2011). Chiasmata promote monopolar attachment of sister chromatids and their co-segregation toward the proper pole during meiosis I. *PLoS Genetics*, *7*(3). https://doi.org/10.1371/journal.pgen.1001329

Huang, M., Hong, M., Hou, X., Zhu, C., Chen, D., Chen, X., Guang, S., & Feng, X. (2022). *H3K9me1/2 methylation limits the lifespan of daf-2 mutants in C. elegans*. 11. https://doi.org/10.7554/eLife

Jih, G., Iglesias, N., Currie, M. A., Bhanu, N. v., Paulo, J. A., Gygi, S. P., Garcia, B. A., & Moazed, D. (2017). Unique roles for histone H3K9me states in RNAi and heritable silencing of transcription. *Nature*, *547*(7664), 463–467. https://doi.org/10.1038/nature23267

Kaukonen, D., Kaukonen, R., Polit, L., Hennessy, B. T., Lund, R., & Madden, S. F. (2020). Analysis of H3K4me3 and H3K27me3 bivalent promotors in HER2+ breast cancer cell lines reveals variations depending on estrogen receptor status and significantly correlates with gene expression. *BMC Medical Genomics*, *13*(1). https://doi.org/10.1186/s12920-020-00749-2

Klass, M. R. (1977). Aging in the nematode Caenorhabditis elegans: Major biological and environmental factors influencing life span. In *Mechanisms of Ageing and Development* (Vol. 6).

Kostrouchova, M., Krause, M., Kostrouch, Z. and Rall, J. E. (1998). CHR3: a Caenorhabditis elegans orphan nuclear hormone receptor required for proper epidermal development and molting. Development 125, 1617-1626.

Kranz, A. L., Jiao, C. Y., Winterkorn, L. H., Albritton, S. E., Kramer, M., & Ercan, S. (2013). Genome-wide analysis of condensin binding in Caenorhabditis elegans. *Genome Biology*, *14*(10), 1–15.https://doi.org/10.1186/gb-2013-14-10-r112

Lai, C. H., Chou, C. Y., Ch'ang, L. Y., Liu, C. S., & Lin, W. C. (n.d.). *Identification of Novel Human Genes Evolutionarily Conserved in Caenorhabditis elegans by Comparative Proteomics*. doi: https://doi.org/10.1101/gr.10.5.703

L'hernault, S. W., & Robertst, T. M. (n.d.). *Cell Biology of Nematode Sperm*. https://doi.org/10.1016/s0091-679x(08)61392-8

Lodish, H. F., Berk, A., Kaiser, C., Krieger, M., Bretscher, A., Ploegh, H. L., Amon, A., & Martin, K. C. (2016). *Molecular cell biology* (Eighth). W.H. Freeman-Macmillan Learning.

Loyola, A., Bonaldi, T., Roche, D., Imhof, A., & Almouzni, G. (2006). PTMs on H3 Variants before Chromatin Assembly Potentiate Their Final Epigenetic State. *Molecular Cell*, *24*(2), 309–316. https://doi.org/10.1016/j.molcel.2006.08.019

Mariño-Ramírez, L., Kann, M. G., Shoemaker, B. A., & Landsman, D. (2005). Histone structure and nucleosome stability. In *Expert Review of Proteomics* (Vol. 2, Issue 5, pp. 719–729). https://doi.org/10.1586/14789450.2.5.719

Morelli, M. A., & Cohen, P. E. (2005). Not all germ cells are created equal: Aspects of sexual dimorphism in mammalian meiosis. In *Reproduction* (Vol. 130, Issue 6, pp. 761–781). https://doi.org/10.1530/rep.1.00865

Morrison, O., & Thakur, J. (2021). Molecular complexes at euchromatin, heterochromatin and centromeric chromatin. *International Journal of Molecular Sciences*, *22*(13). https://doi.org/10.3390/ijms22136922

Padeken, J., Zeller, P., Towbin, B., Katic, I., Kalck, V., Methot, S. P., & Gasser, S. M. (2019). Synergistic lethality between BRCA1 and H3K9me2 loss reflects satellite derepression. *Genes and Development*, *33*(7–8), 436–451. https://doi.org/10.1101/gad.322495.118

Pawlowski, W. P., & Cande, W. Z. (2005). Coordinating the events of the meiotic prophase. In *Trends in Cell Biology*(Vol. 15, Issue 12, pp. 674–681). https://doi.org/10.1016/j.tcb.2005.10.005

Phillips, C. M., Wong, C., Bhalla, N., Carlton, P. M., Weiser, P., Meneely, P. M., & Dernburg, A. F. (2005). HIM-8 binds to the X chromosome pairing center and mediates chromosome-specific meiotic synapsis. *Cell*, *123*(6), 1051–1063. https://doi.org/10.1016/j.cell.2005.09.035

Ragle, J. M., Aita, A. L., Morrison, K. N., Martinez-Mendez, R., Saeger, H. N., Ashley, G. A., Johnson, L. C., Schubert, K. A., Shakes, D. C., & Ward, J. D. (2020). The conserved molting/circadian rhythm regulator NHR-23/ NR1F1 serves as an essential co-regulator of C. elegans spermatogenesis. *Development (Cambridge)*, *147*(22). https://doi.org/10.1242/dev.193862

Riddle, D. L., Blumenthal, T., Meyer, B. J., Priess, J. R. (1997). C. elegans II. 2nd edition. Cold Spring Harbor (NY): Cold Spring Harbor Laboratory Press. https://www.ncbi.nlm.nih.gov/books/NBK19997

Samson, M., Jow, M. M., Wong, C. C. L., Fitzpatrick, C., Aslanian, A., Saucedo, I., Estrada, R., Ito, T., Park, S. kyu R., Yates, J. R., & Chu, D. S. (2014). The Specification and Global Reprogramming of Histone Epigenetic Marks during Gamete Formation and Early Embryo Development in C. elegans. *PLoS Genetics*, *10*(10), 17–21. https://doi.org/10.1371/journal.pgen.1004588

Schedl, T., & Kimble, J. (1988). *fog-2, a Germ-Line-Specific Sex Determination Gene Required for Hermaphrodite Spermatogenesis in Caenorhabditis elegans*. https://academic.oup.com/genetics/article/119/1/43/5997696

Schulenburg, H., & Félix, M. A. (2017). The natural biotic environment of Caenorhabditis elegans. *Genetics*, *206*(1), 55–86. https://doi.org/10.1534/genetics.116.195511

Seidel, H. S., Smith, T. A., Evans, J. K., Stamper, J. Q., Mast, T. G., & Kimble, J. (2018). C. elegans germ cells divide and differentiate in a folded tissue. *Developmental Biology*, *442*(1), 173–187. https://doi.org/10.1016/j.ydbio.2018.07.013

Shakes, D. C. (2011). For male Caenorhabditis elegans, sperm activation is a "Just-in-time" event. In *PLoS Genetics* (Vol. 7, Issue 11). https://doi.org/10.1371/journal.pgen.1002392

Shakes, D. C., Wu, J. C., Sadler, P. L., LaPrade, K., Moore, L. L., Noritake, A., & Chu, D. S. (2009). Spermatogenesis-specific features of the meiotic program in Caenorhabditis elegans. *PLoS Genetics*, *5*(8). https://doi.org/10.1371/journal.pgen.1000611

Smith, J. R., & Stanfield, G. M. (2012). A seminal fluid protease activates sperm motility in C. elegans males. *Worm*, *1*(3), 151–154. https://doi.org/10.4161/worm.19502

Snyman, M., Huynh, T. v., Smith, M. T., & Xu, S. (2021). The genome-wide rate and spectrum of EMS-induced heritable mutations in the microcrustacean Daphnia: on the prospect of forward genetics. *Heredity*, *127*(6), 535–545. https://doi.org/10.1038/s41437-021-00478-x

Spiller, C., Koopman, P., & Bowles, J. (2017). Sex Determination in the Mammalian Germline. *Annual Review of Genetics*, 43. https://doi.org/10.1146/annurev-genet-120215

Stear, J. H., & Roth, M. B. (2002). Characterization of HCP-6, a *C. elegans* protein Required To Prevent Chromosome Twisting and Merotelic Attachment. *Genes Dev, 16*(12), 1498–1508.https://doi.org/10.1101/gad.989102

Stiernagle, T. (2006). Maintenance of C. elegans. In *WormBook : the online review of C. elegans biology* (pp. 1–11). https://doi.org/10.1895/wormbook.1.101.1

Strome, S., Kelly, W. G., Ercan, S., & Lieb, J. D. (2014). Regulation of the X chromosomes in Caenorhabditis elegans. *Cold Spring Harbor Perspectives in Biology*, *6*(3). https://doi.org/10.1101/cshperspect.a018366

Towbin, B. D., González-Aguilera, C., Sack, R., Gaidatzis, D., Kalck, V., Meister, P., Askjaer, P., & Gasser, S. M. (2012). Step-wise methylation of histone H3K9 positions heterochromatin at the nuclear periphery. *Cell*, *150*(5), 934–947. https://doi.org/10.1016/j.cell.2012.06.051

Woodhouse, R. M., Buchmann, G., Hoe, M., Harney, D. J., Low, J. K. K., Larance, M., Boag, P. R., & Ashe, A. (2018). Chromatin Modifiers SET-25 and SET-32 Are Required for Establishment but Not Long-Term Maintenance of Transgenerational Epigenetic Inheritance. *Cell Reports*, *25*(8), 2259-2272.e5. https://doi.org/10.1016/j.celrep.2018.10.085

Wu, D., Rea, S. L., Cypser, J. R., & Johnson, T. E. (2009). Mortality shifts in Caenorhabditis elegans: Remembrance of conditions past. *Aging Cell*, *8*(6), 666–675. https://doi.org/10.1111/j.1474-9726.2009.00523.x

Xiao, R., Zhang, B., Dong, Y., Gong, J., Xu, T., Liu, J., & Xu, X. Z. S. (2013). A genetic program promotes C. elegans longevity at cold temperatures via a thermosensitive TRP channel. *Cell*, *152*(4), 806–817. https://doi.org/10.1016/j.cell.2013.01.020

Zhang, B., Xiao, R., Ronan, E. A., He, Y., Hsu, A. L., Liu, J., & Xu, X. Z. S. (2015). Environmental Temperature Differentially Modulates C. elegans Longevity through a Thermosensitive TRP Channel. *Cell Reports*, *11*(9), 1414–1424. https://doi.org/10.1016/j.celrep.2015.04.066

Appendix A

PREVIOUS WORK ON HTAS-1 AND HCP-6

HTAS-1, one of the investigated candidate genes, is a sperm-specific histone H2A variant involved in chromatin remodeling during spermatogenesis. HTAS-1 is only expressed during spermatogenesis in both males and hermaphrodites (Samson et al., 2014). We measured bivalent length in *htas-1(ok1573)* deletion mutant males, reasoning that if bivalent length changes, it should be specific to males. As previously mentioned, *htas-1(ok1573)* deletion mutant bivalent length of spermatocytes is reduced (*htas-1(ok1573)*: 2.61 μm**, Figure 1.4**), whereas that of oocytes showed no significant difference compared to wild type (Salvitti, L. unpublished data). To examine the effect of reduced spermatocytes bivalent length on embryonic performance, I conducted embryonic viability assays and mating assays on *htas-1(ok1573)* hermaphrodites. Embryonic viability results revealed there is a significant difference between *htas-1(ok1573)* and wild type in hermaphrodites self mating and when *htas-1(ok1573)* hermaphrodites are mated with wild type males (Selfing: N2 is 98.4%, *htas-1(ok1573)* is 97.0%, $p = 0.5211$; Mating: N2 is 98.3%, *htas-1(ok1573)* is 99.8%, $p = 0.1680$, **Figure S1**), however, only two EVA trials were completed for *htas-1(ok1573)* and additional trials may reveal that there is no significant difference from wild type.

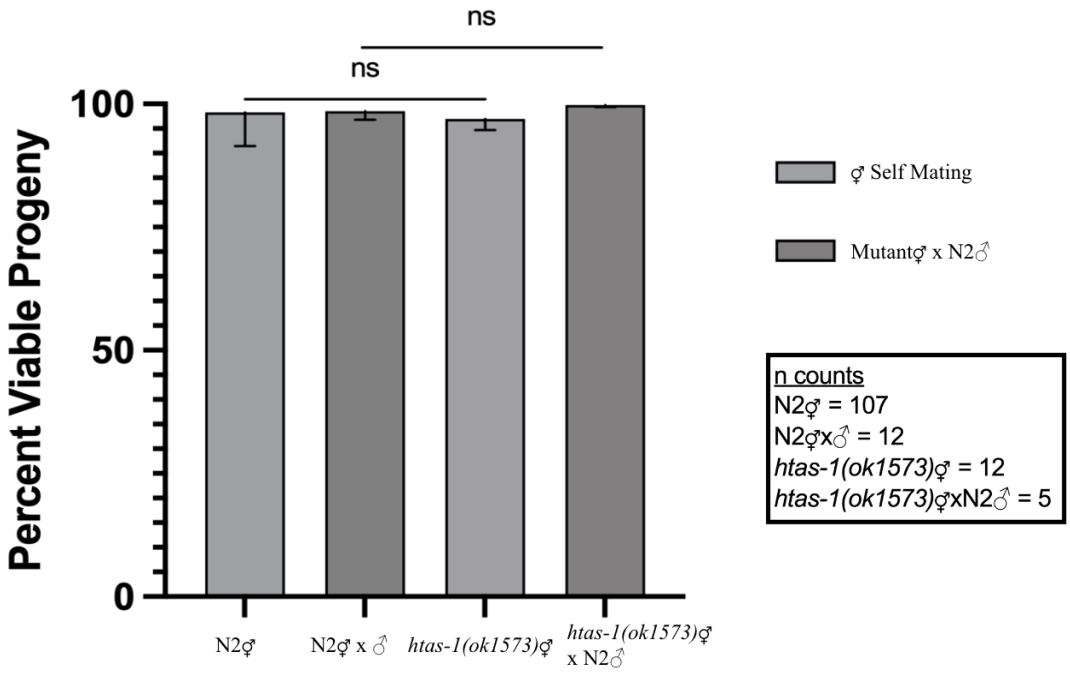

Figure A.1: Loss of HTAS-1 does not affect embryonic viability. Embryonic viability assay were performed to calculate the percentage of the embryonic viability of hermaphrodites self-mating and cross mating in wild type and *htas-1(ok1573)* at 20℃. Error bar represents the standard deviation of the average percent of embryonic viability. Statistical analysis performed by unpaired t.test.

I have also investigated holocentric protein 6 (HCP-6), which is a subunit of Condensin II and its relationship to chromosome structure during late meiotic prophase I. For these experiments, I used the *hcp-6(mr17)* mutant strain. The *mr17* allele of *hcp-6* is a single nucleotide change, G to A transition, at position 3073 in the protein-coding region, which leads to a missense mutation [conversion of glycine 1024 to glutamic acid (Stear and Roth, 2002)]. *hcp-6(mr17)* is a temperature sensitive mutant that at the nonpermissive temperature results in failure of chromosome condensation and embryonic lethality (Herbette et al., 2020). Unfortunately, I could not locate the mutation on the gene sequence of the *hcp-6(mr17)* mutant strain through sequencing, therefore I was not confident that the phenotypes I observed were due to *hcp-6* defects or some other background mutation so this project was not continued.

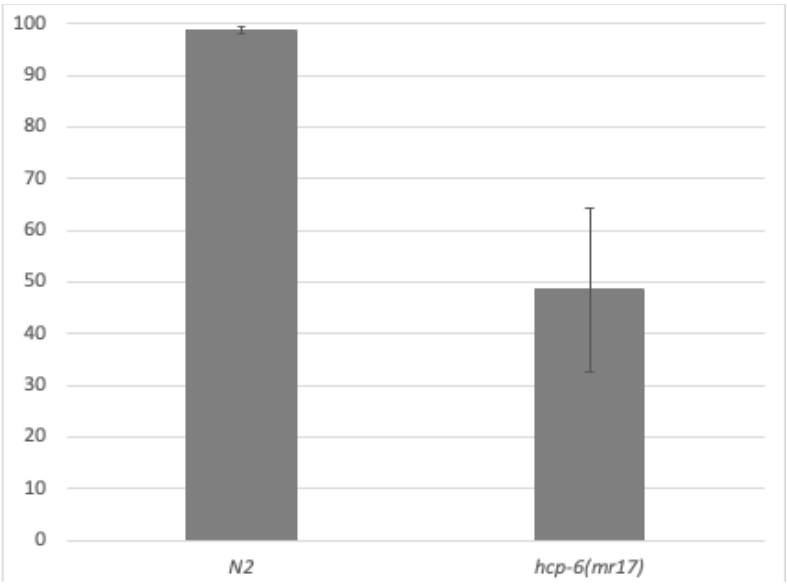

Figure A.2: **Loss of *hcp-6(mr17)* causes a reduction in embryonic viability at 24℃.** Embryonic viability assays were performed to calculate the average percent of embryonic viability of N2 (wild type) and *hcp-6(mr17)* (temperature sensitive mutant). Error bars represent the standard deviation of the average percent of embryonic viability. The number of hermaphrodites scored for progeny were N2= 30 and *hcp-6(mr17)*= 30. $p<0.05$. Data collected by summer intern Deonna Beard of Delaware State University.

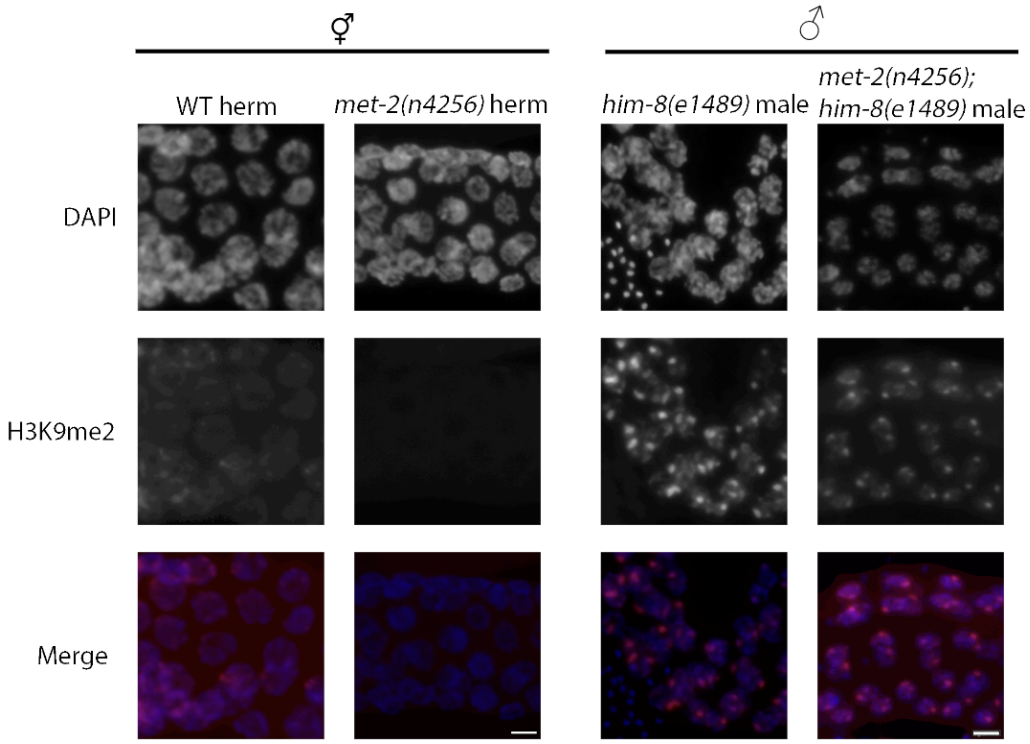

Figure A.3: H3K9me2 is detected on chromosomes within pachytene in spermatogenesis. Germline pachytene of wild type and *met-2(n4256)* hermaphrodites stained with H3K9me2 in red (middle panels) and DAPI in blue (top panels) shown in the left two columns; Germline pachytene of wild type and *met-2(n4256)* males stained with H3K9me2 in red (middle panels) and DAPI in blue (top panels) shown in the right two columns. Scale bar = 5 μm.